National Taiwan University

Taipei,
November 22, 2011

ASIAA/CCMS/IAMS/NTU-Phys Joint Colloquia

From STEM-EELS to multi-dimensional and multi-signal electron microscopy

Christian Colliex
Laboratoire de Physique des Solides, Bldg 510
Université Paris Sud, 91405, Orsay, France
christian.colliex@u-psud.fr

cnrs dépasser les frontières

LPS ORSAY Laboratoire de Physique des Solides · UMR 8502 Université Paris sud bât 510 · 91405 Orsay cedex

UNIVERSITÉ PARIS SUD Comprendre le monde, construire l'avenir®

Outline

Signals, instrumentation and methods for STEM EELS

Atomically resolved elemental and bonding maps

Mapping plasmons and EM fields

When electrons and photons team up

JEM

Journal of Electron Microscopy **60(Supplement 1)**: S161–S171 (2011)
doi: 10.1093/jmicro/dfr028

60th Anniversary Issue: Physical

From electron energy-loss spectroscopy to multi-dimensional and multi-signal electron microscopy

Christian Colliex*

Laboratoire de Physique des Solides (UMR CNRS 8502), Université Paris Sud, Bldg. 510, 91405 Orsay, France

Electron – Matter interactions

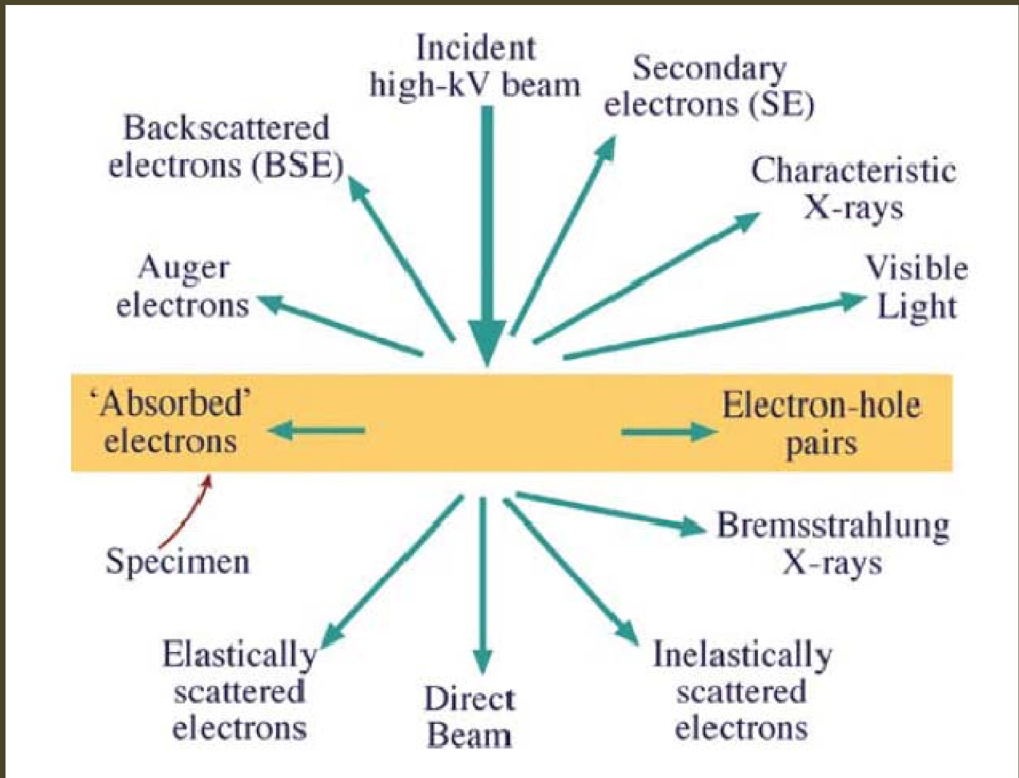

Secondary Event

vs.

Primary Event

Transmission Electron Microscopy - A Textbook for Material Science
David Williams and Barry Carter, Fig. 1.3, page 7.

Working modes for an transmission electron microscope

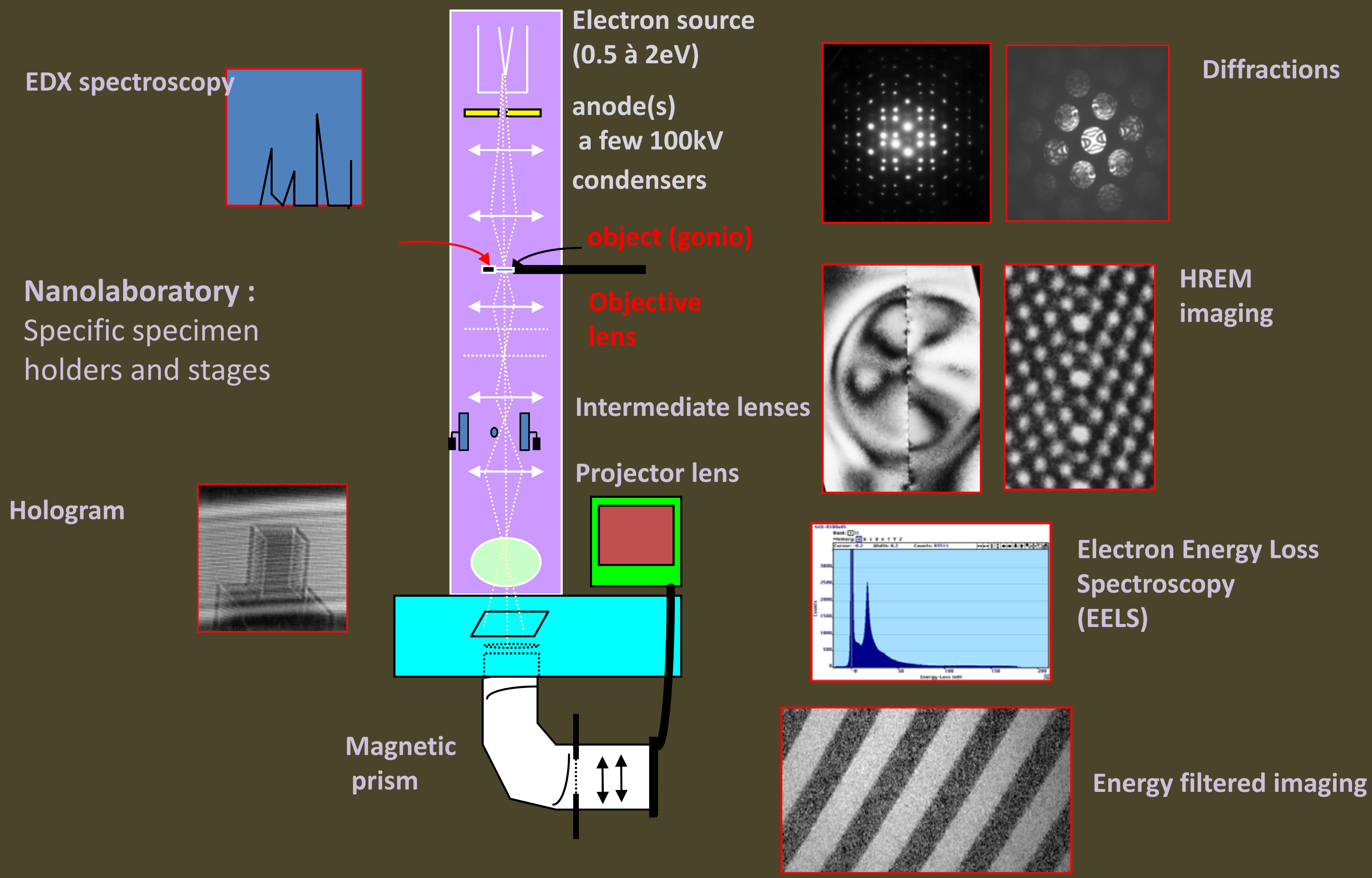

STEMs with EELS analysers at Orsay

1980 - 20xx

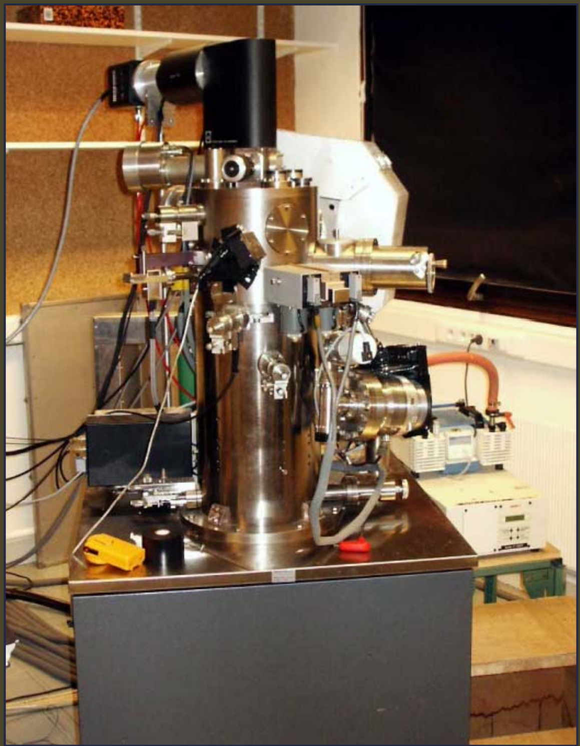

VG HB 501

2008 - 2011

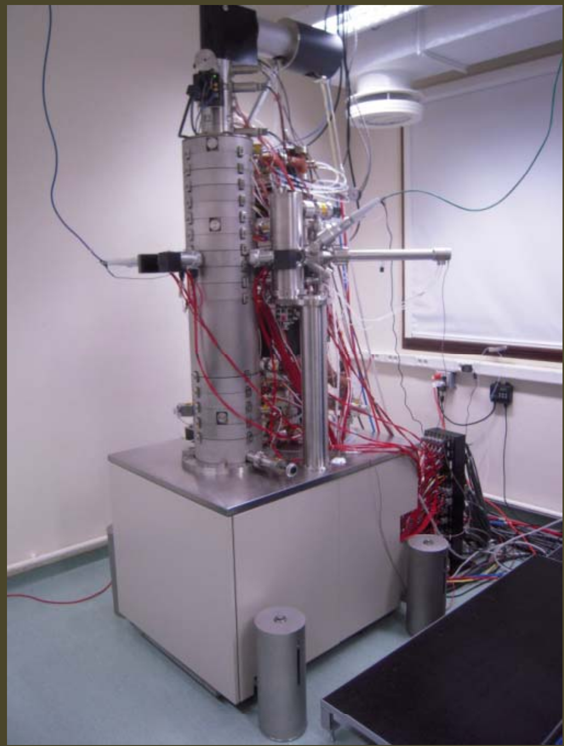

NION UltraSTEM 100

2011 - 20xx

NION UltraSTEM 200

EELS spectrum-image at Orsay

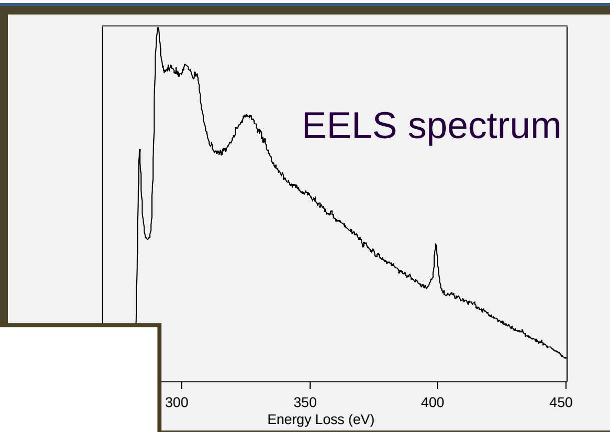

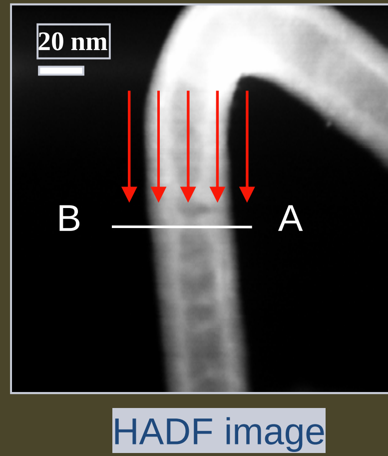

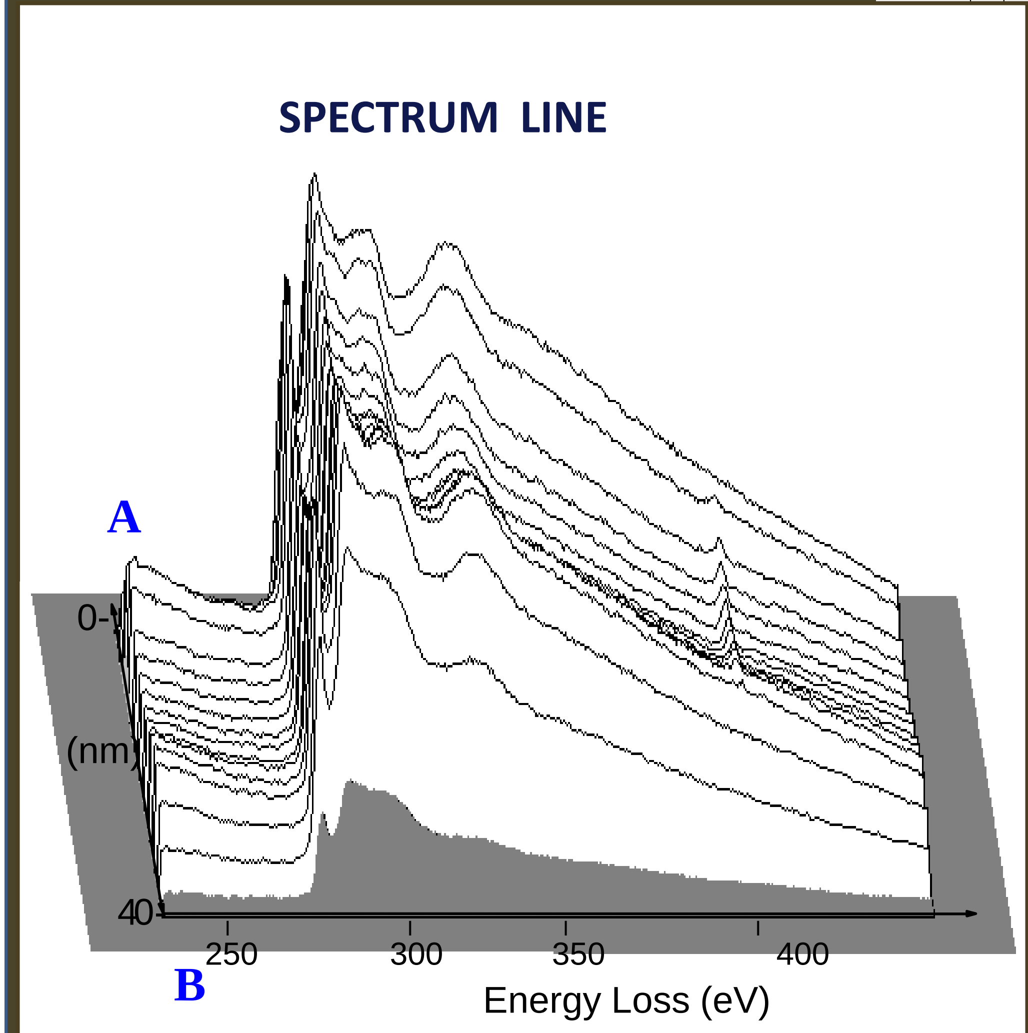

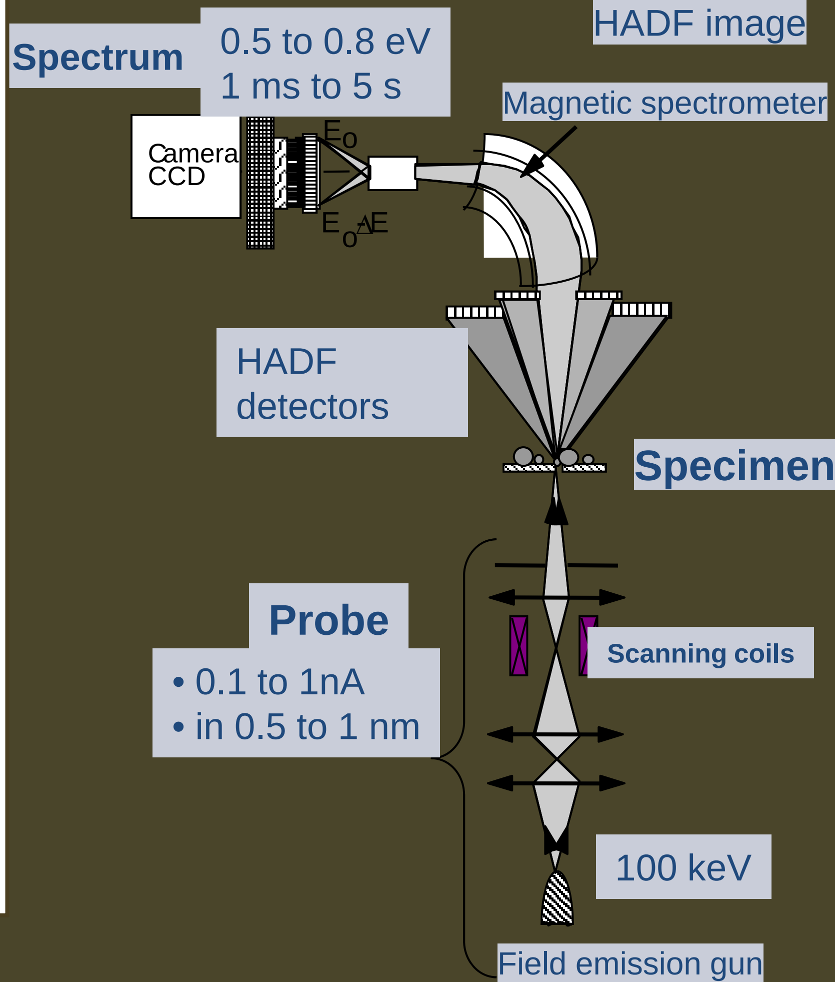

Multi-dimensional microscopy in a composite space (x,y position, E energy and t time)

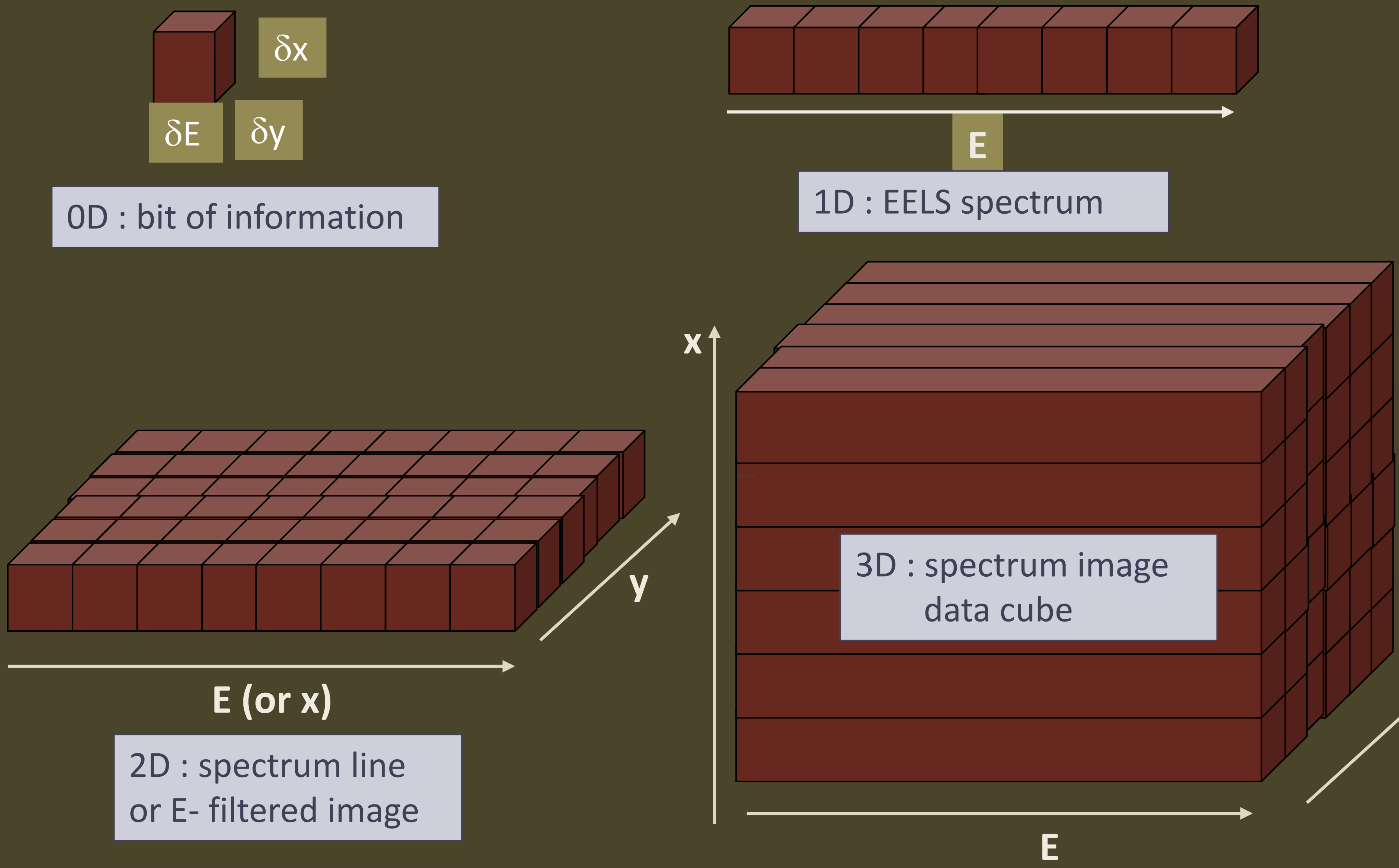

An electron microscope for the aberration-corrected era

O.L. Krivanek*, G.J. Corbin, N. Dellby, B.F. Elston, R.J. Keyse, M.F. Murfitt, C.S. Own, Z.S. Szilagyi, J.W. Woodruff

Nion Co., 1102 8th Street, Kirkland, WA 98033, USA

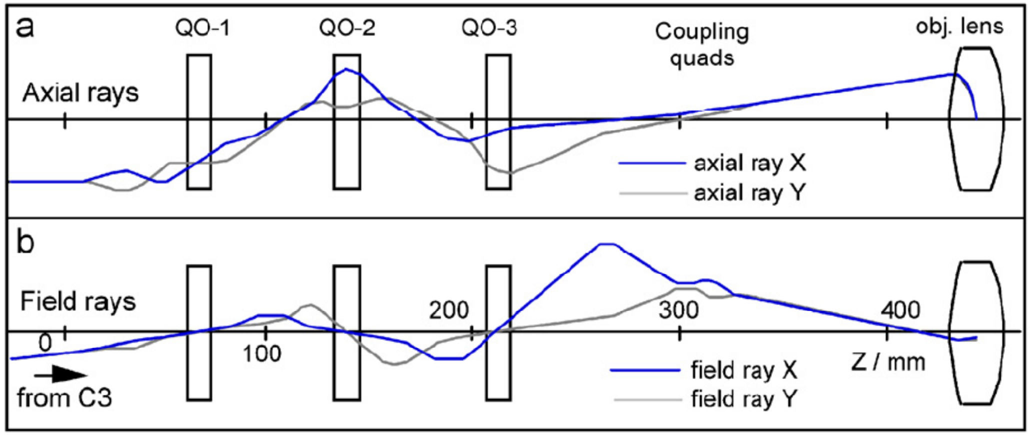

Fig. 3. Axial (a) and field (b) trajectories through the C_3/C_5 corrector.

Use of C_s correctors to reduce probe size or to increase probe current :

i) <1 Å probe size at 100 kV, <0.7 Å at 200 kV

ii) 200 pA of current in a 1.4 Å probe

iii) 1 nA current in a 2.3 Å probe

Fig. 6. The theoretical probe size of a 200 kV C_3/C_5 corrected STEM giving an aberration-limited probe of 50 pm FWHM, as a function of the probe current for two different brightnesses. $B = 3 \times 10^{13}$ A / (m^2 sr) is representative of CFEG systems, $B = 5 \times 10^{12}$ A / (m^2 sr) is representative of Schottky systems [14] (at 200 kV).

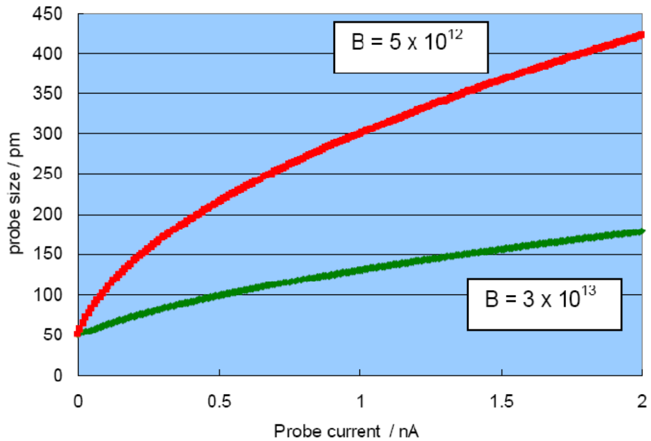

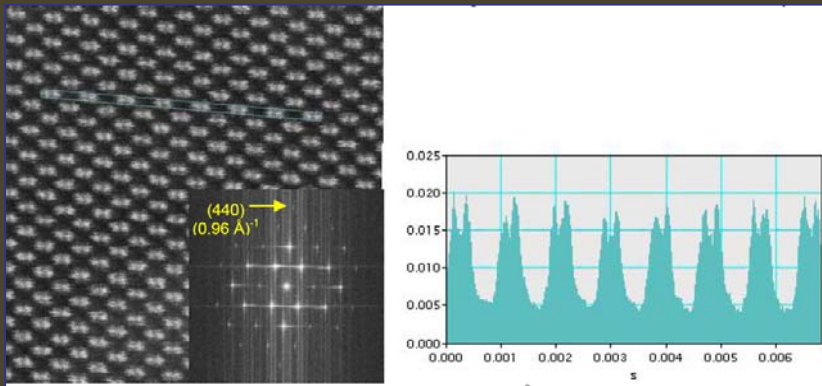

57pA Si dumbbells, with contrast transfer to below 1Å.

Orsay Nion U-STEM 100 acceptance tests

New UltraSTEM for aberration-corrected nanoanalysis (delivered in Orsay in 2008)

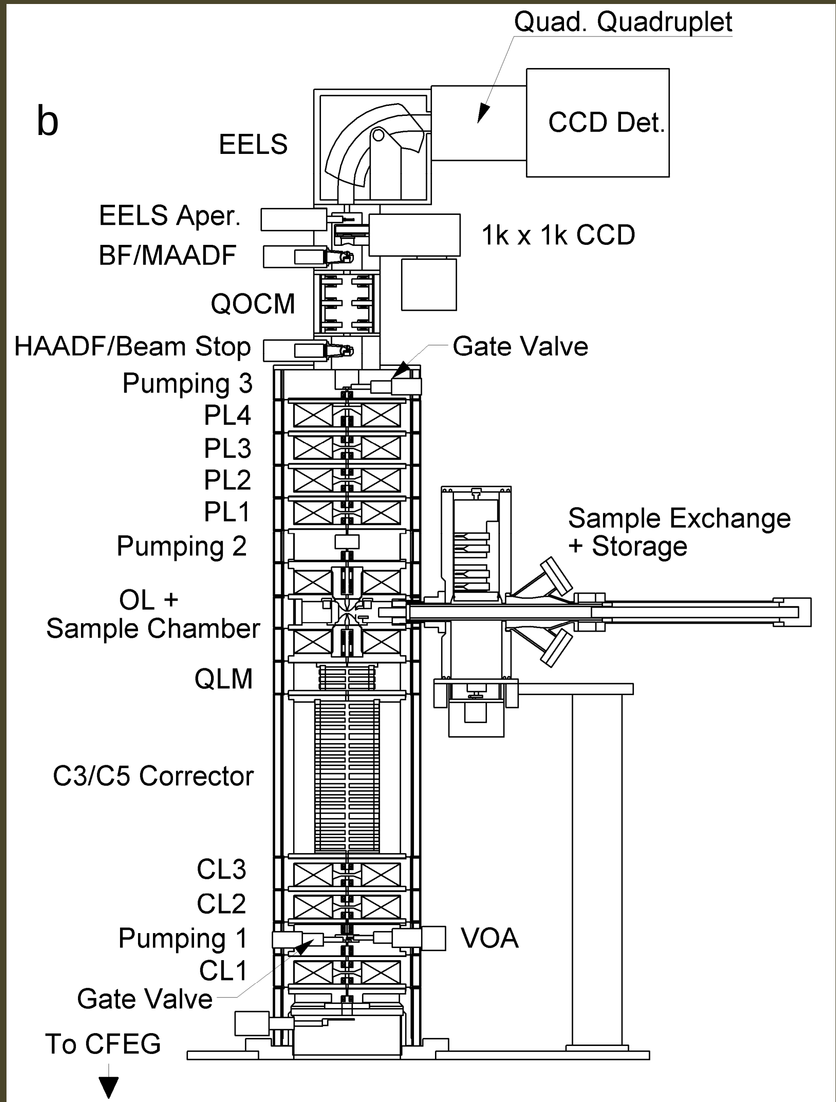

The column is built from modules that all have the same mechanical interface and are 100% interchangeable.

Each module has triple magnetic plus acoustic shielding.

Emphasis is on small probe formation and efficient coupling into detectors.

Everything including sample exchange can be operated remotely.

nion

Nion UltraSTEM 200 performance at Orsay

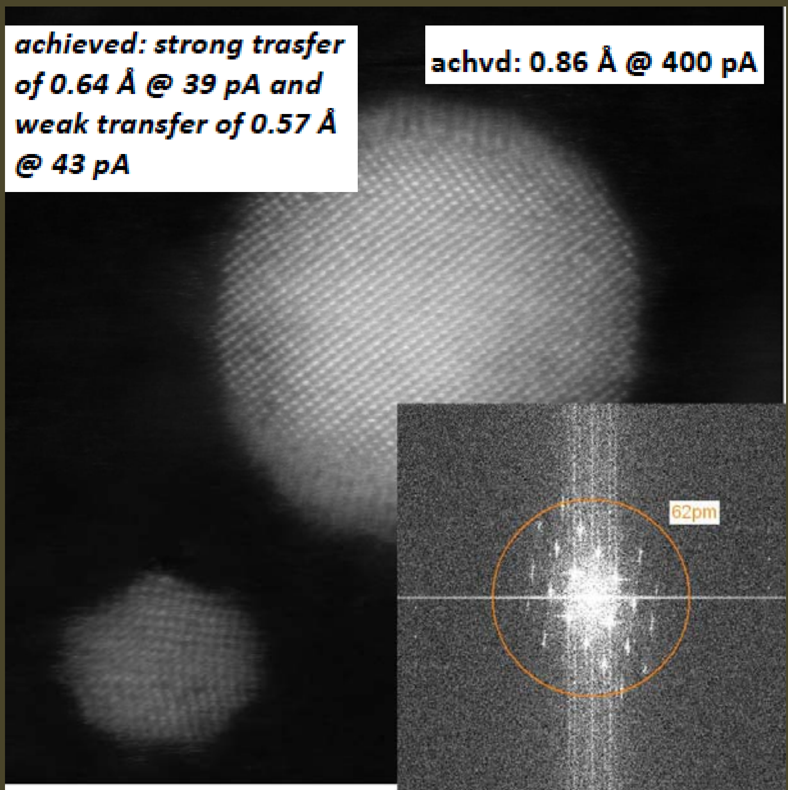

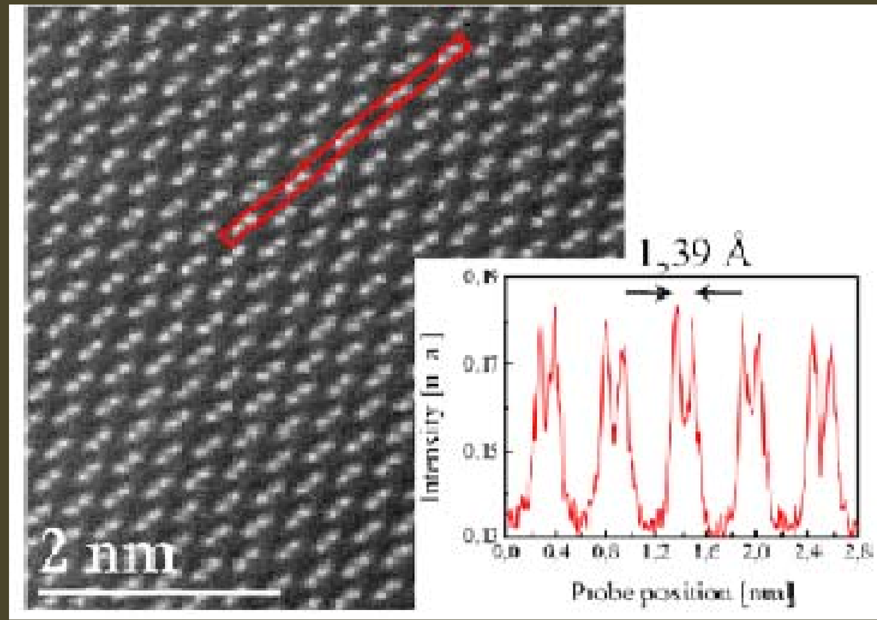

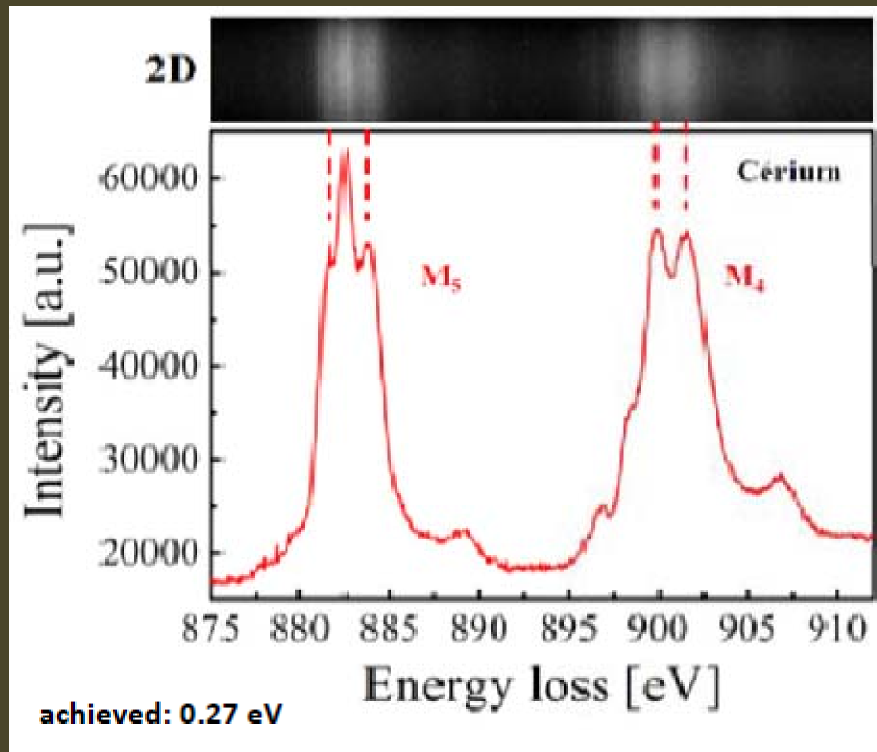

Imaging molecules containing heavy atoms

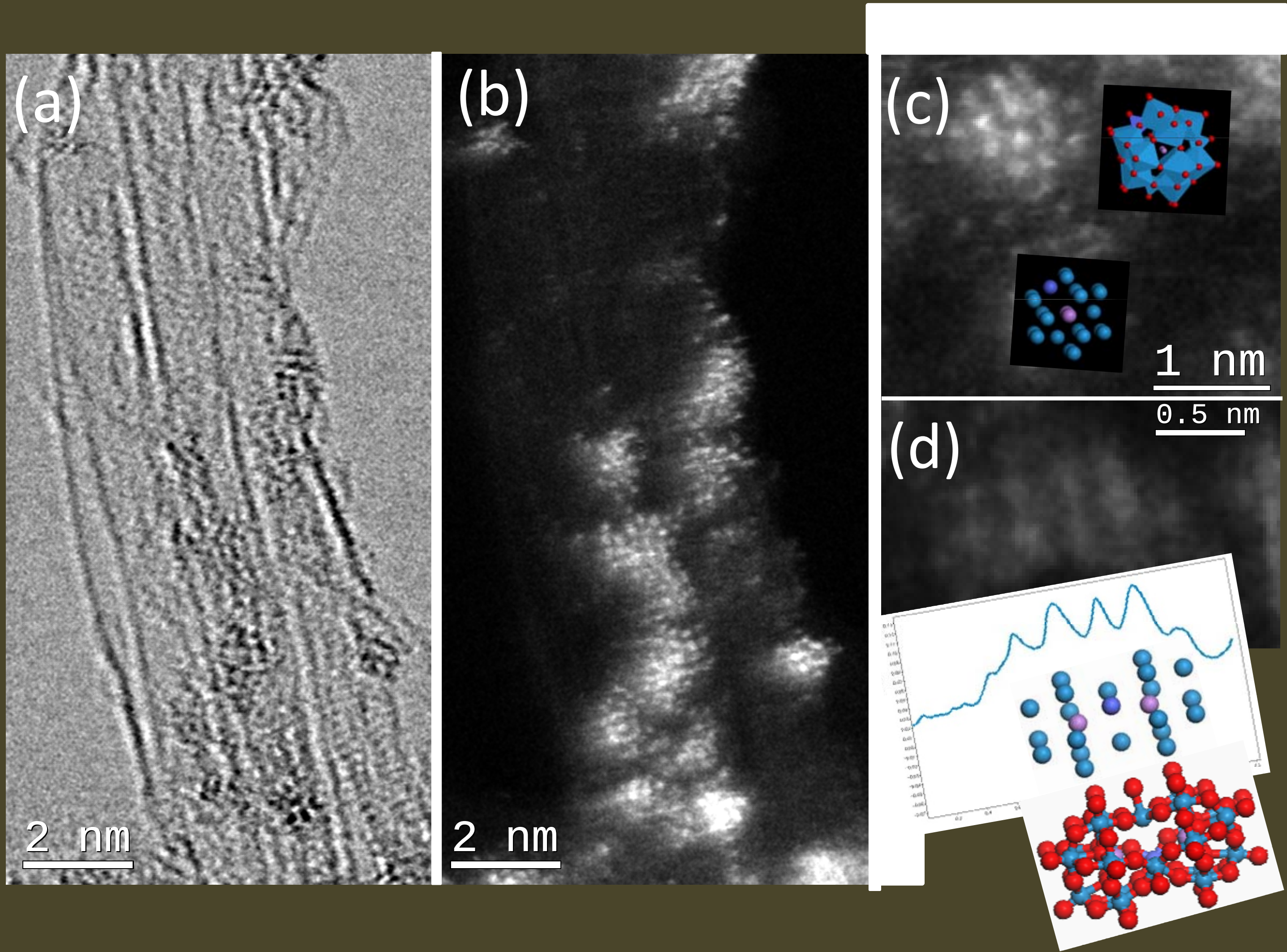

polyoxometalate (POM; $As_2W_{20}O_{70}Co(H_2O)$) molecules grafted on C-SWNT
courtesy A. Gloter, Orsay (2011)

BN monolayer with i

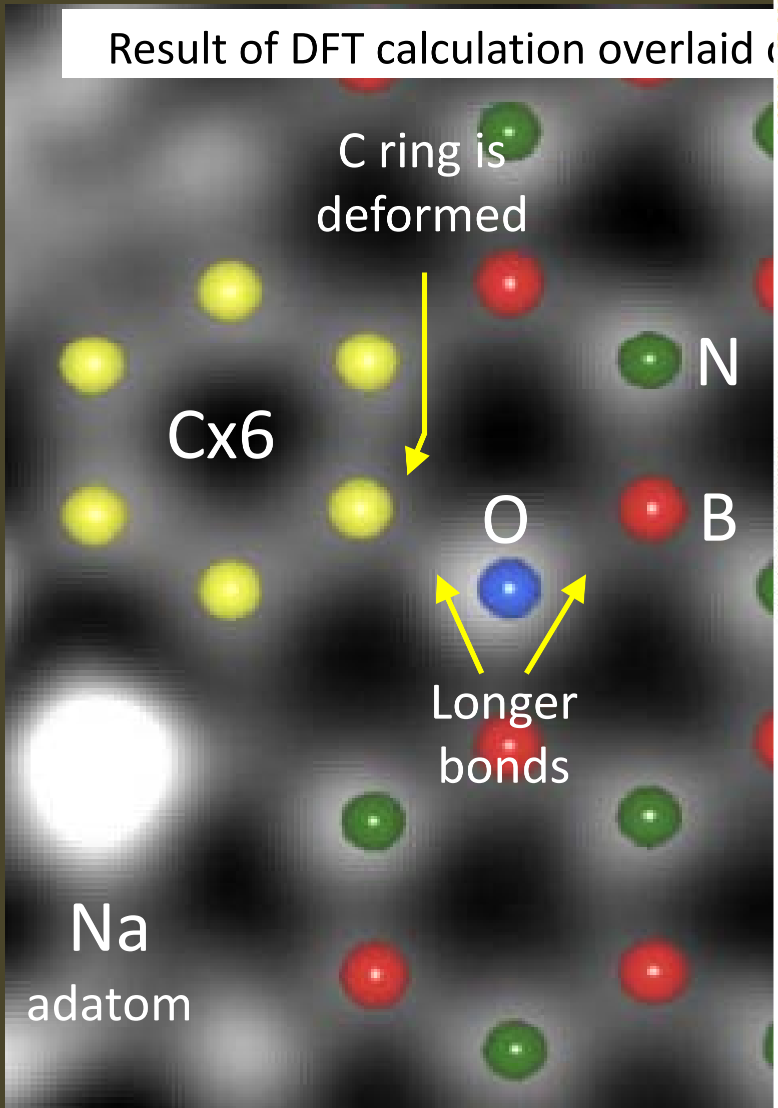

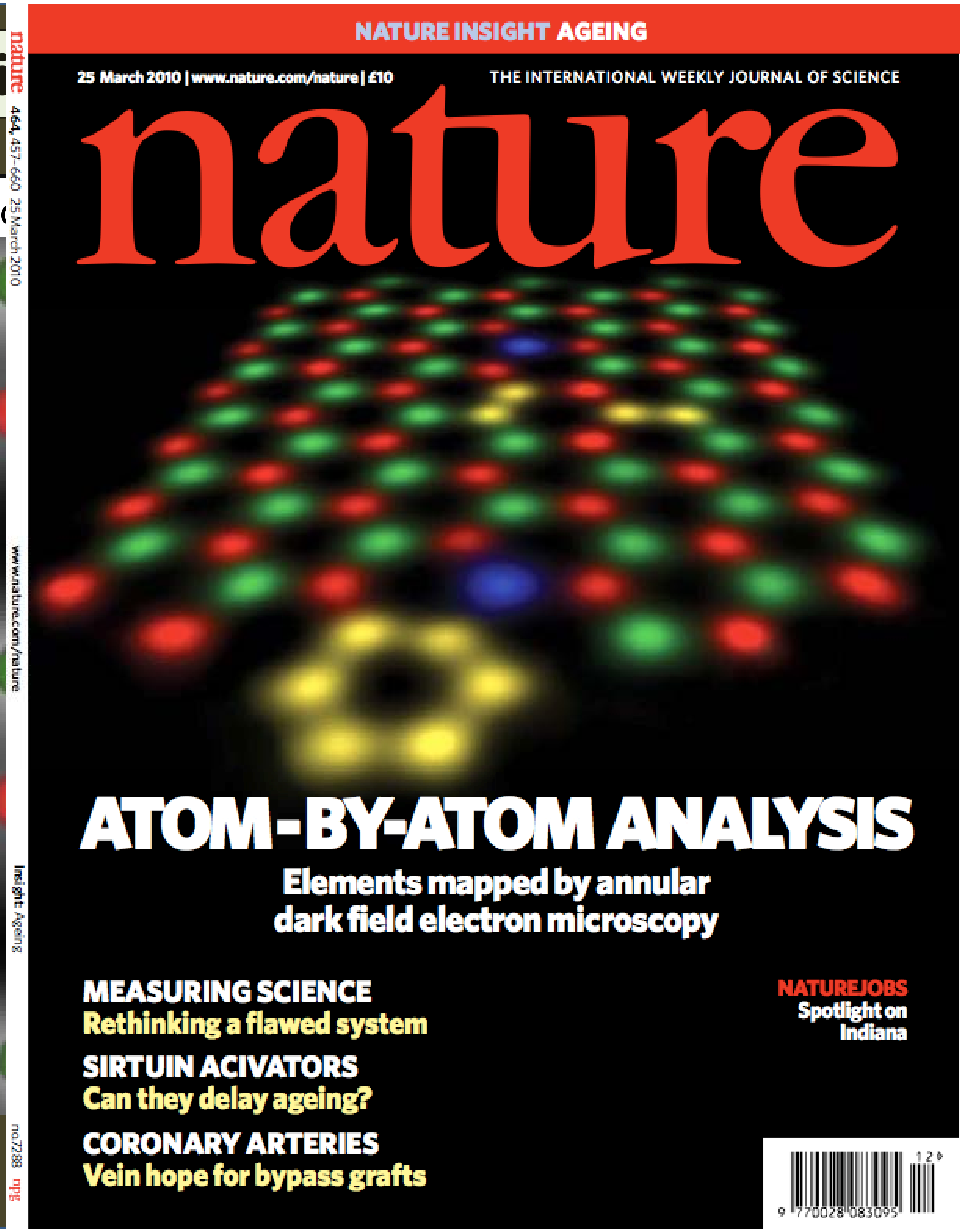

Si substituting for C in monolayer graphene

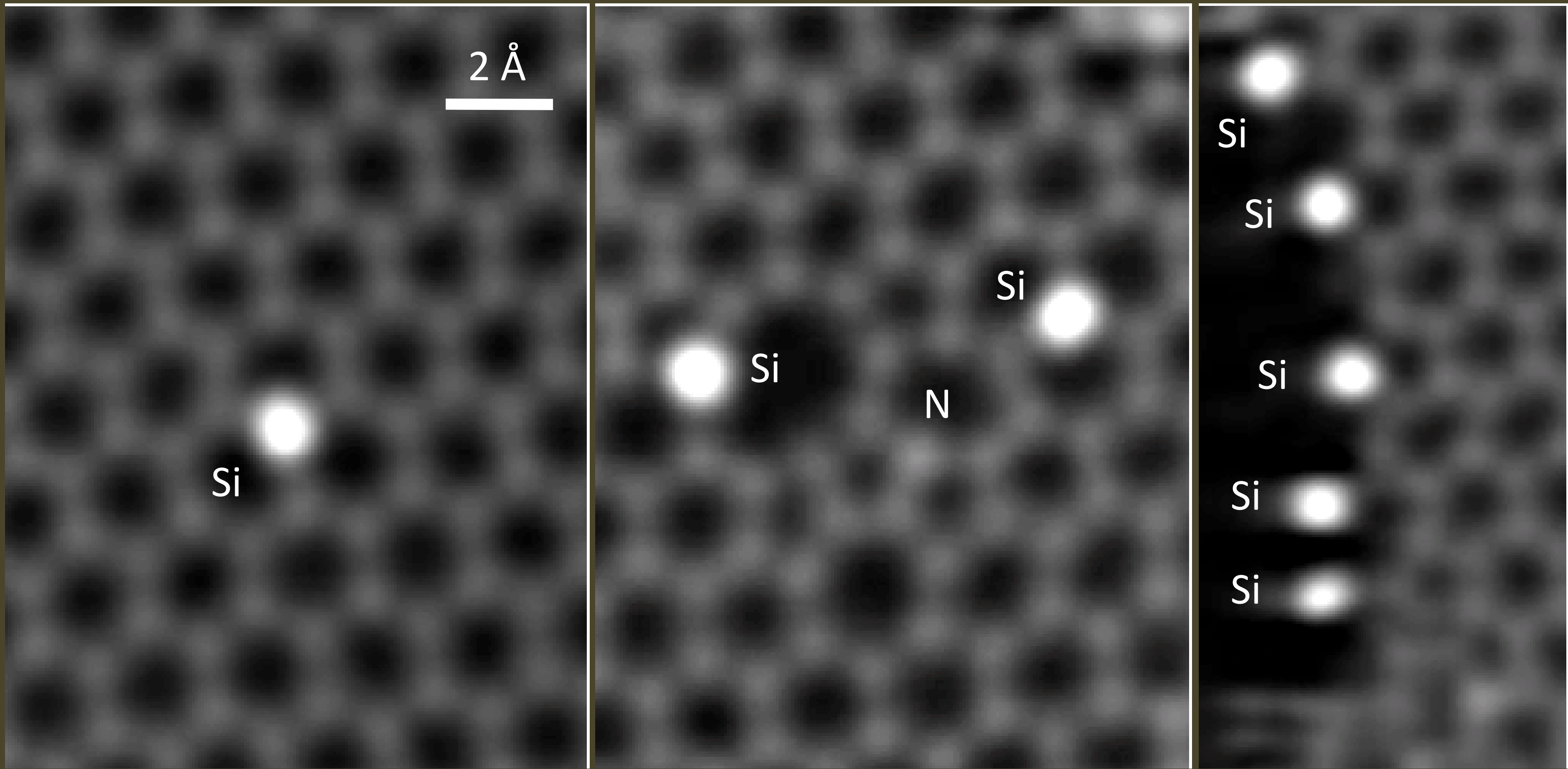

Si in topologically correct graphene

Si at and near topological defects

Si at graphene's edge

Medium angle annular dark field (MAADF) images.
Nion UltraSTEM100 at ORNL, 60 kV. Image courtesy Matt Chisholm, ORNL, sample courtesy Venna Krisnan and Gerd Duscher, U. of Tennessee.

Si substituting for C: 2 structures are possible

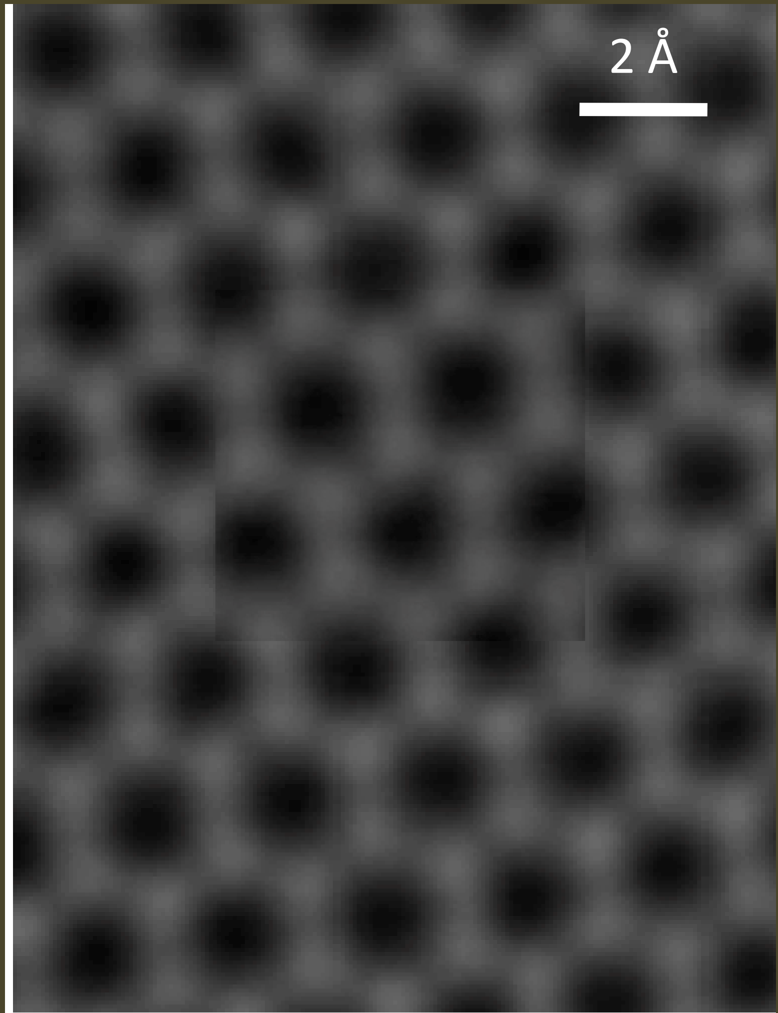

Si in defect-free graphene strains (and buckles) the foil.
(courtesy Matt Chisholm)

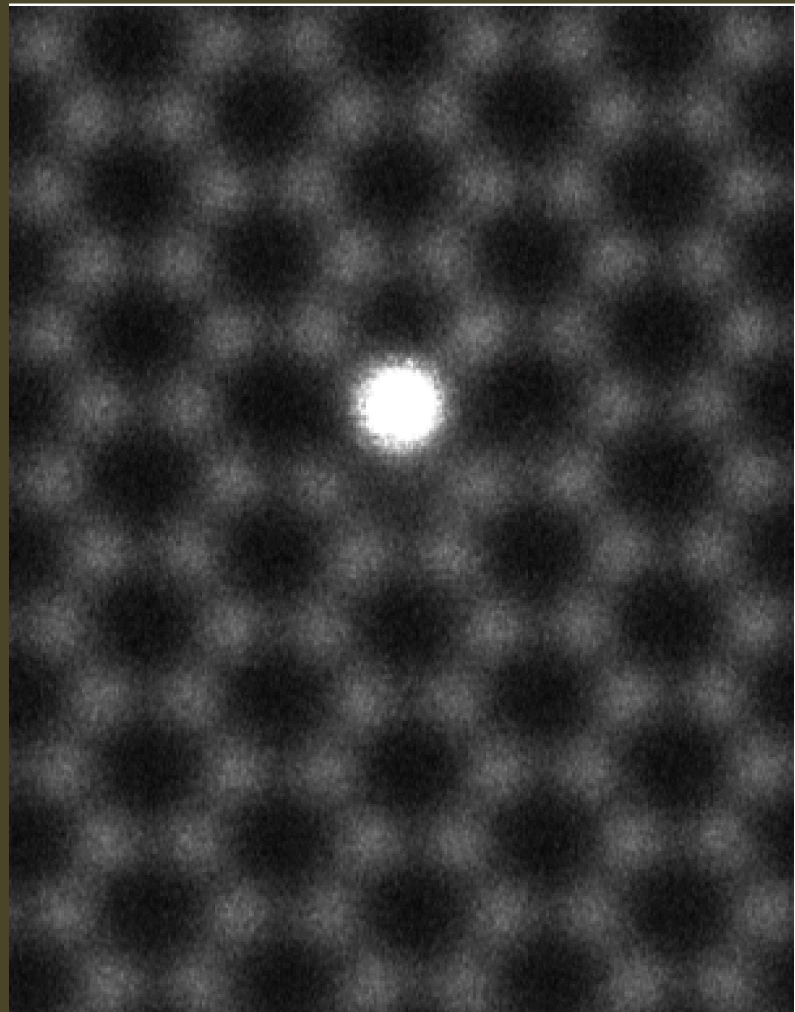

Si in defective, but less strained graphene is more stable. (15 images added together, no other processing,
courtesy Juan-Carlos Idrobo)

EELS spectroscopy : spectral domains

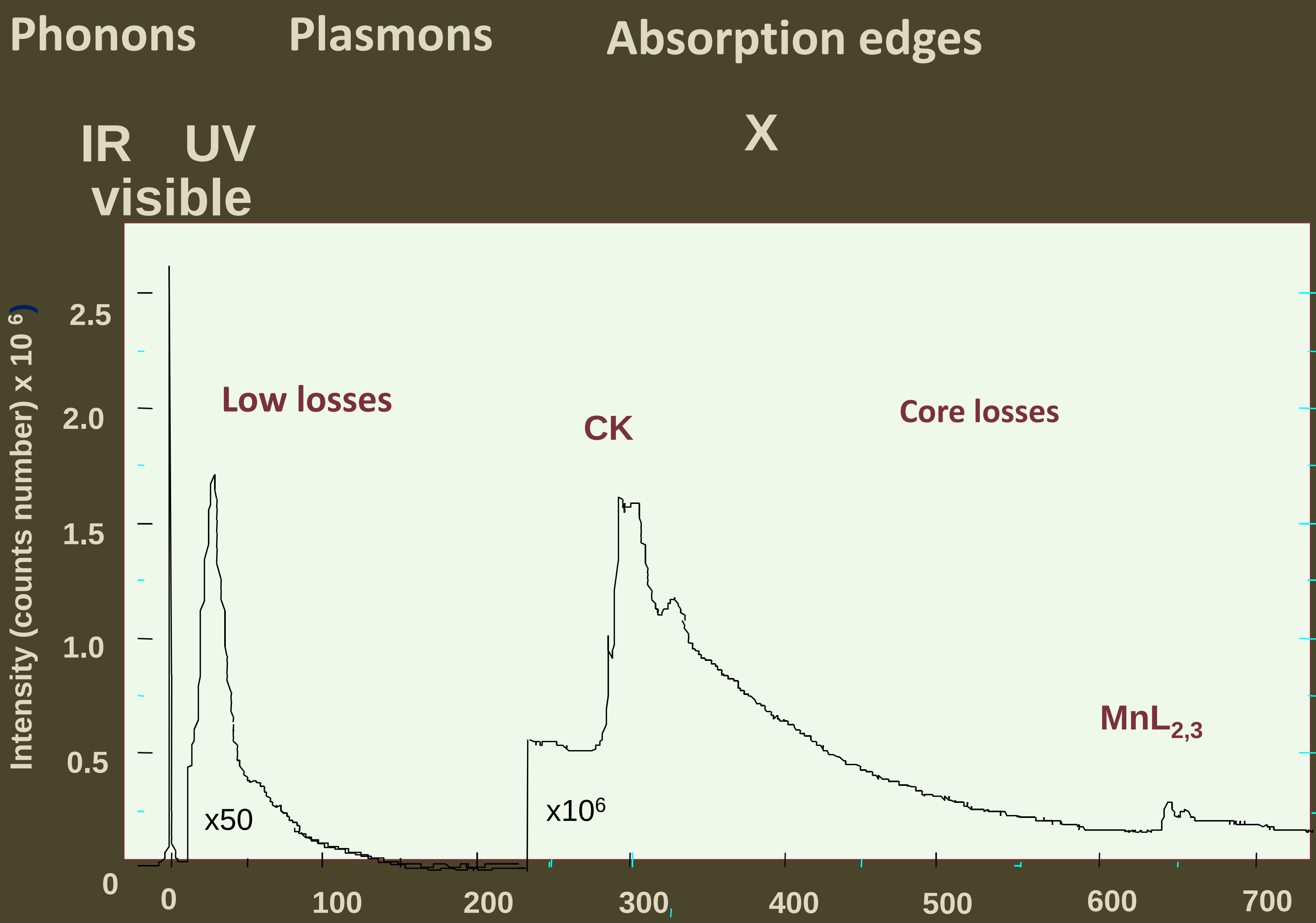

EELS: Involved electron populations and associated transitions

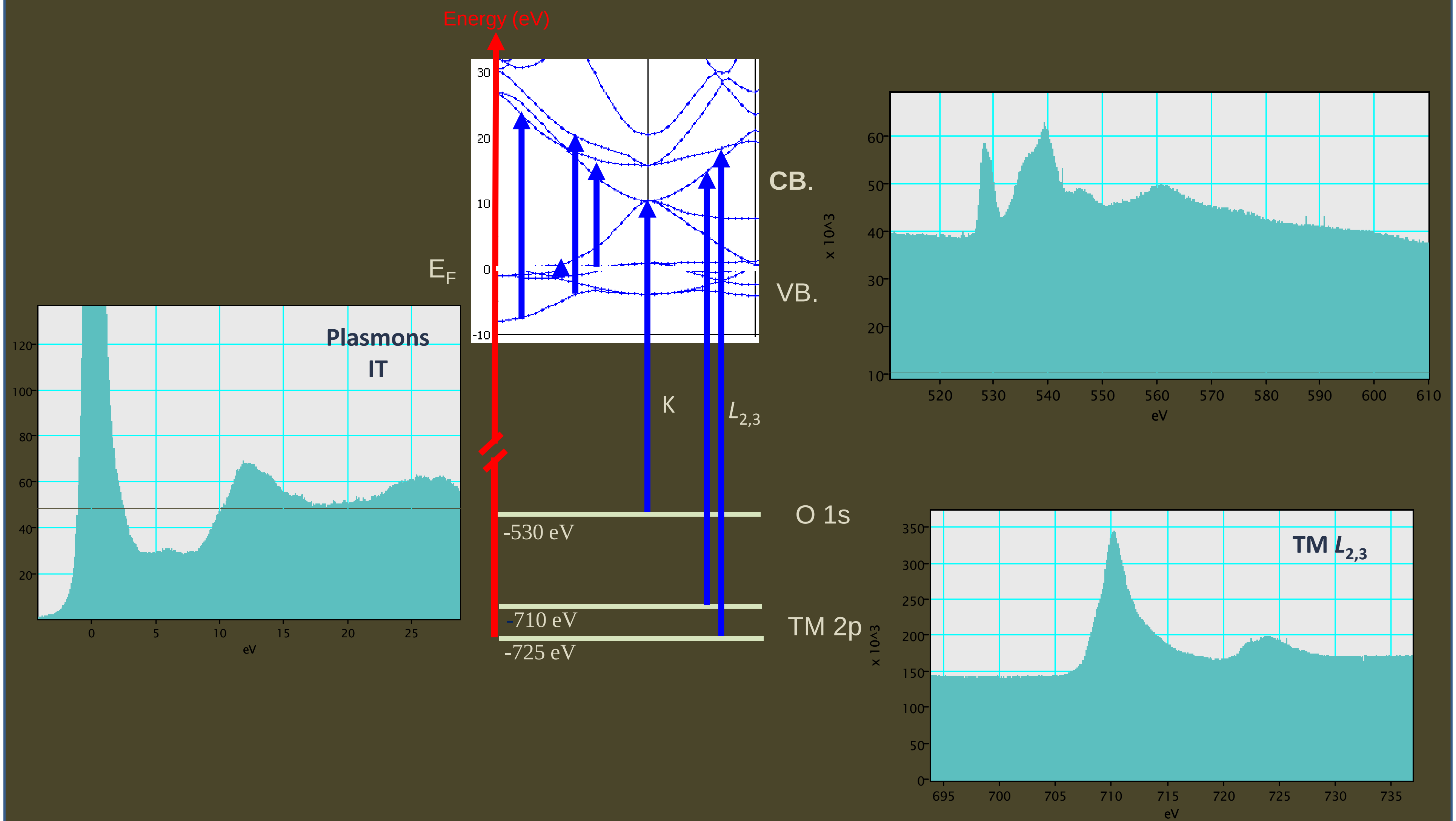

EELS gives informations on the electronic structure

EELS spectroscopy : spectral domains

Low energy-loss domain

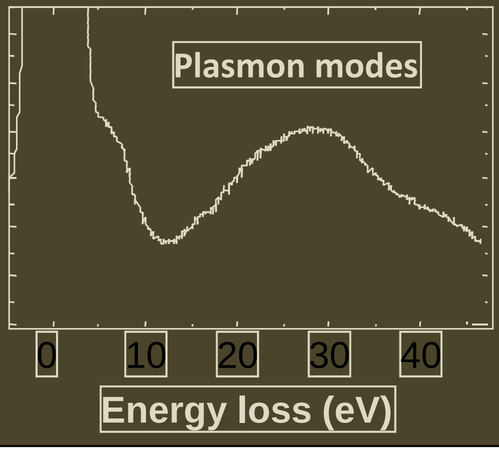

Core energy-loss domain

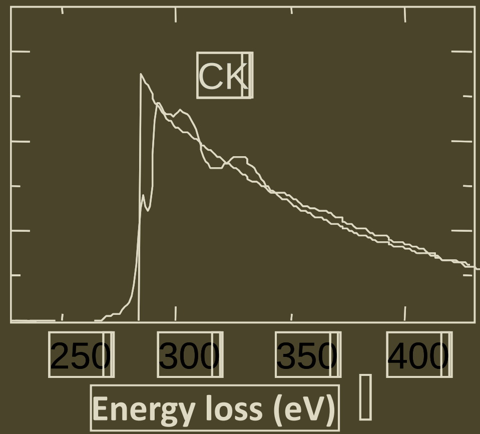

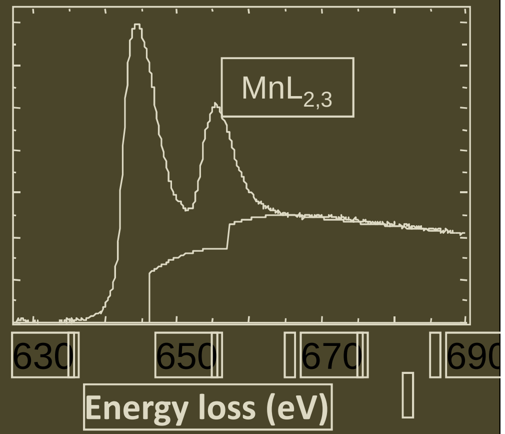

Map different physical parameters, electronic, optical or magnetic, which are especially important for electronic industries

Requires instruments adapted to measure the properties of interest at the relevant scale

→ Towards t

Map with high accuracy the nature, the position and bonding of the atoms responsible for the structural properties of real materials (defects, interfaces, nanomaterials)

Requires instruments with best spatial and energy resolutions

0.1 eV)

In all cases, develop the theory for interpreting spectroscopical data, i.e. a physics of excited states

Absorption edges domain : three types of information

- **Identification of elements**
- **Elementary quantification**
- **Study of the unoccupied electron states distribution**

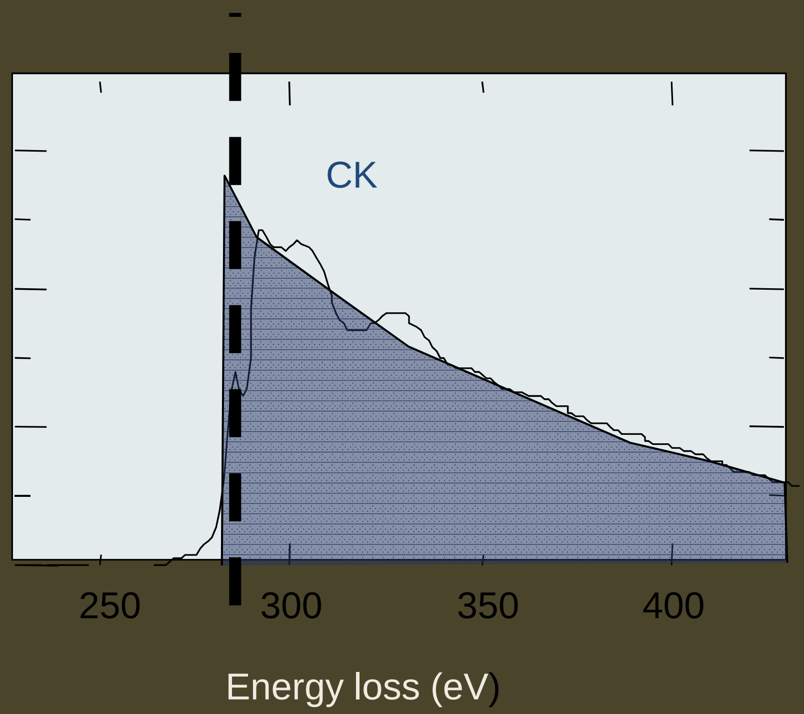

Quantitative elemental analysis

Characteristic signal : proportional to the number of atoms per unit area for the element detected in the analysed area

$$S = ct.\ I\ N\ \sigma$$

Atomic concentration ratios:

$$\frac{N_A}{N_B} = \frac{S_A}{S_B} \times \frac{\sigma_B}{\sigma_A}$$

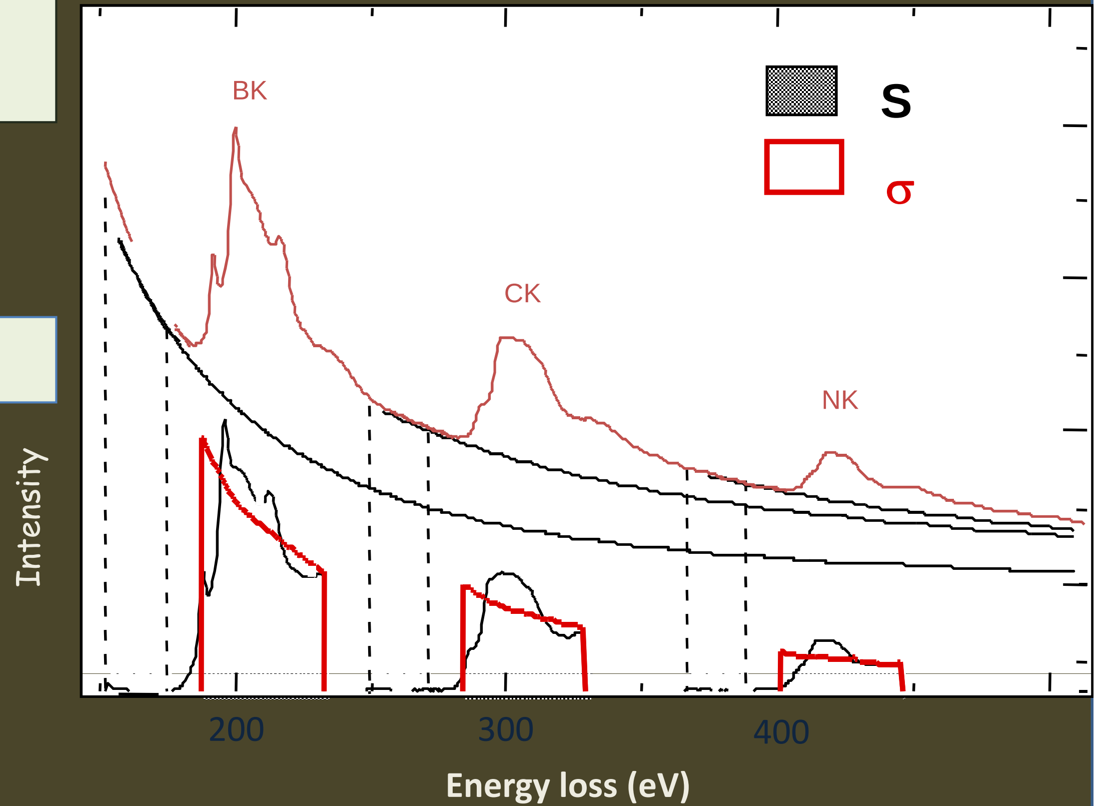

EELS core-level spectroscopy: elemental and bonding maps with atomic resolution

1. Individual atoms
2. Crystalline structures and interfaces
3. Application to Tunnel ElectroMagneto Resistance – TEMR

Single atom identification (signal/noise criteria)

Peapods :

$Gd@C_{82}@SWCNT$

Element selective single-atom imaging

A : HREM image

B : Schematic presentation

C : Superposed maps of the Gd N45 and C K signals extracted from a 32x128 pixels spectrum-image (C in blue, Gd in red)

K. Suenaga et al., Science (2000)

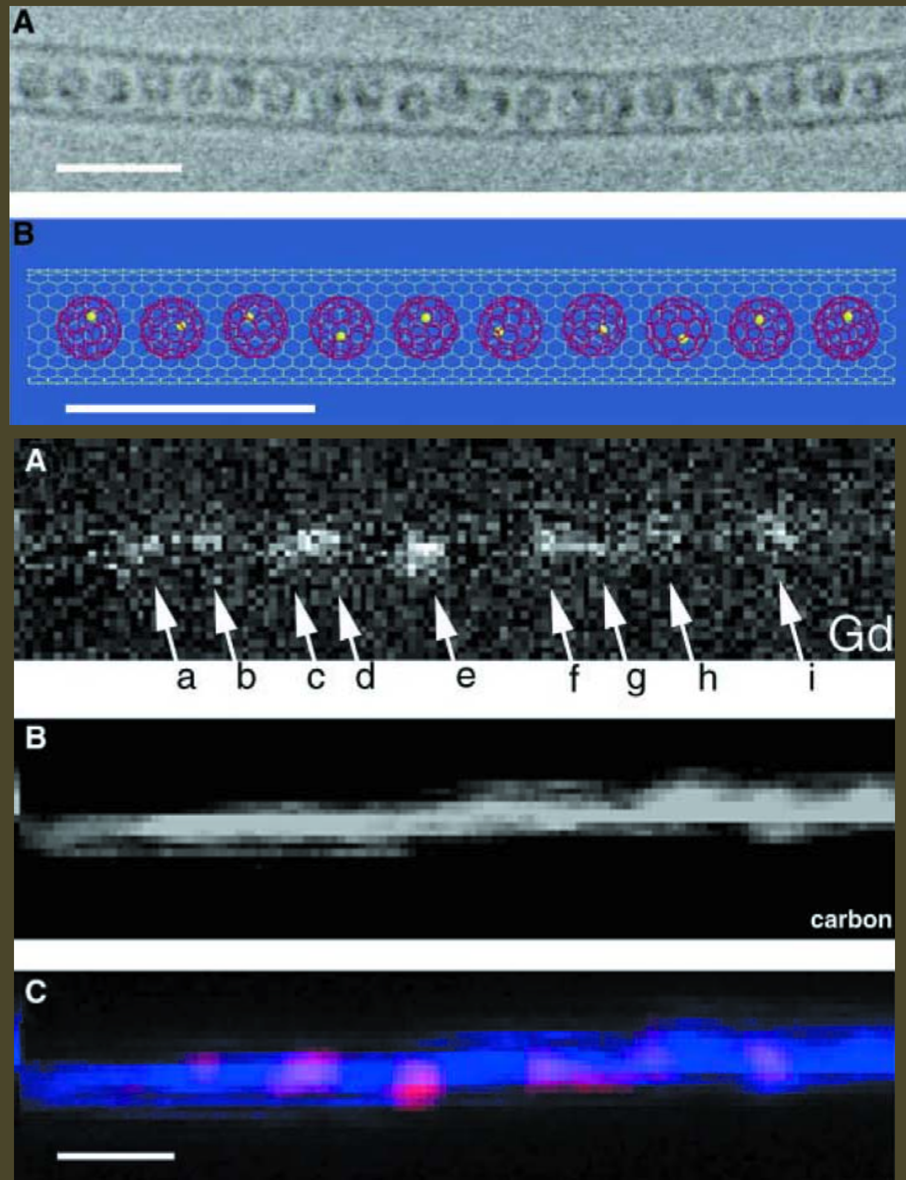

STEM imaging of peapods at 30 and 60 kV with Delta corrector

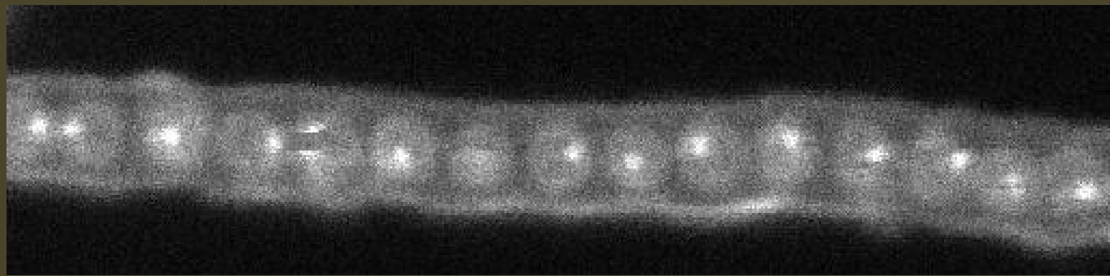

30kV

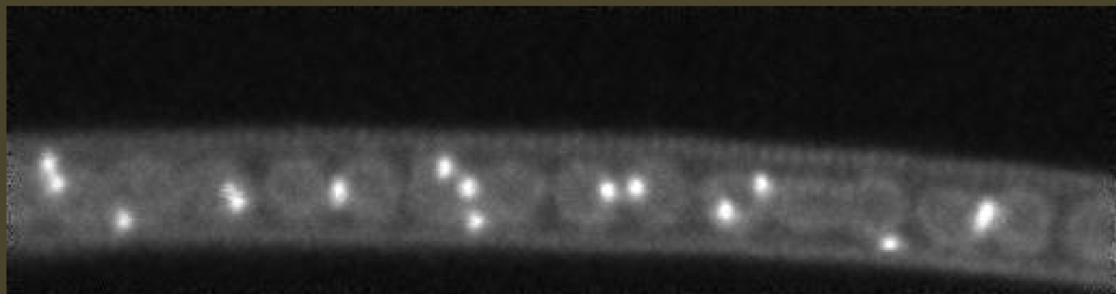

60kV

Damage drastically reduced at 30kV

Courtesy Suenaga, Sawada & Sasaki (2010)

Single atom imaging by STEM-EELS at *low voltage* with the delta corrector

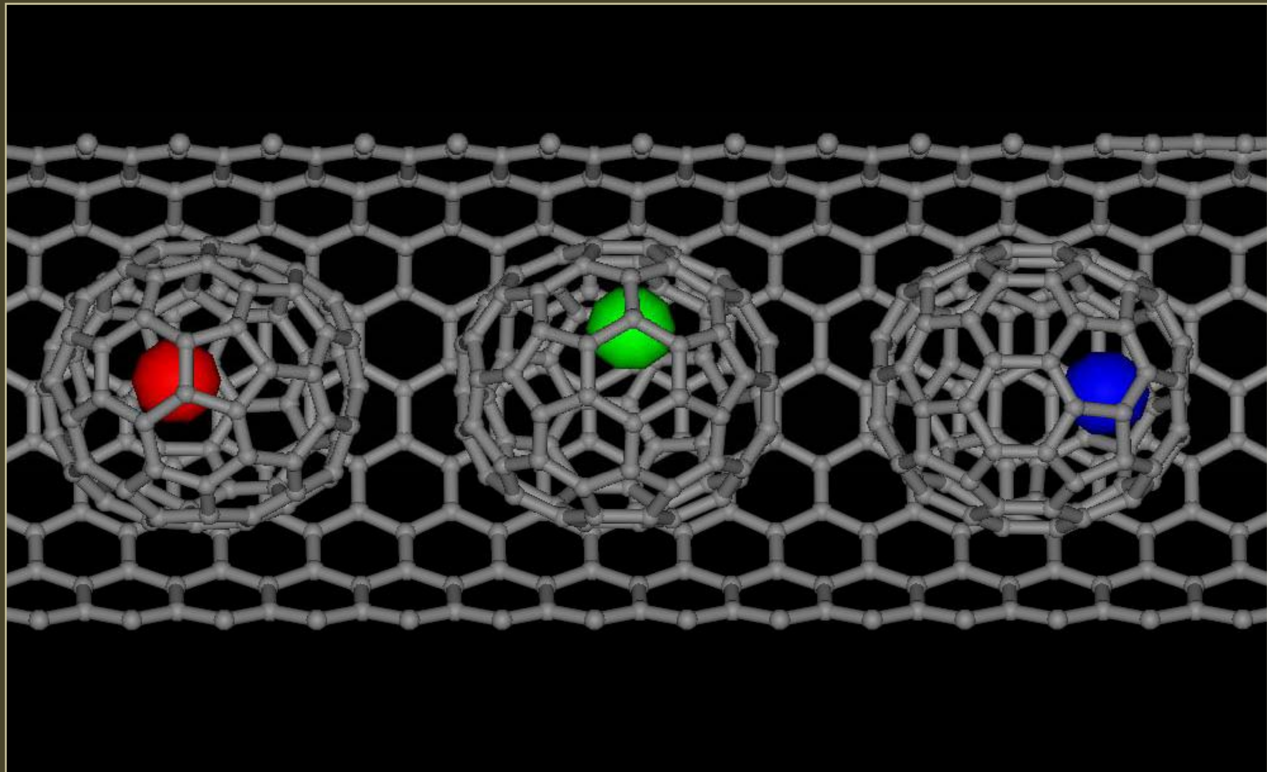

Endohedral fullerenes
M@C82 (M= La, Ce, Er)
Iizumi and Okazaki

Atom by atom labeling at 60kV

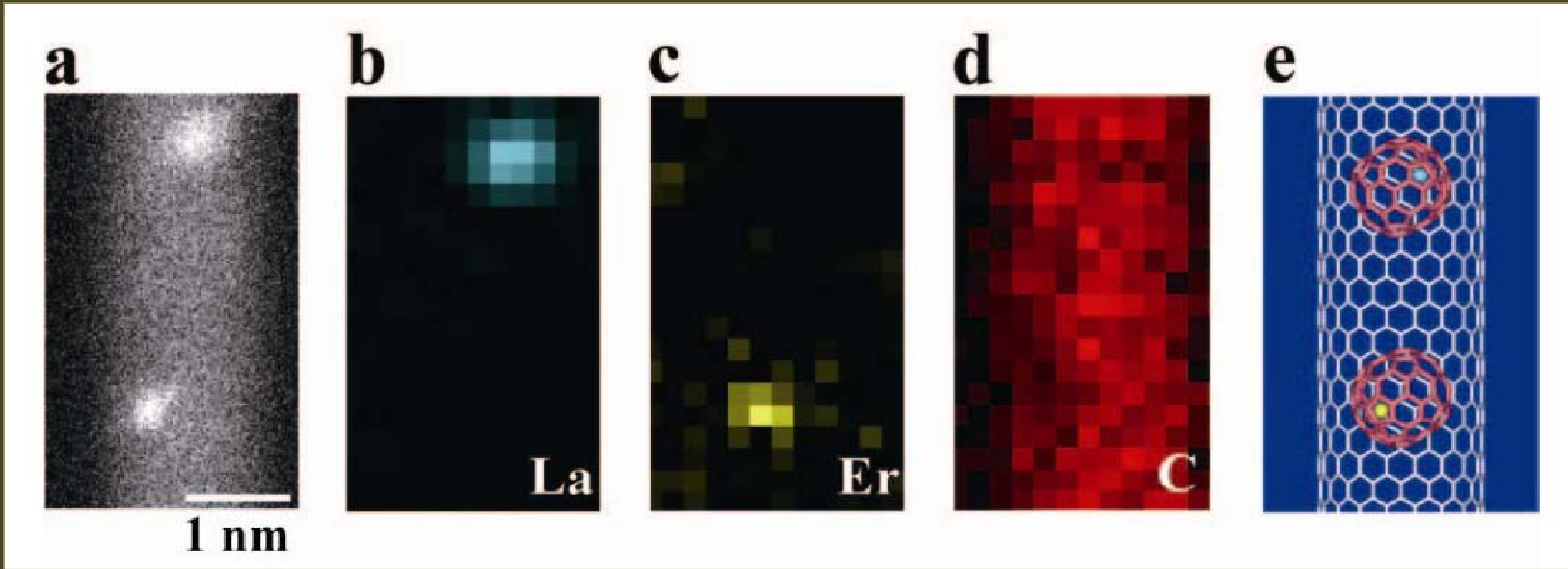

Courtesy K. Suenaga (AIST, Tsukuba, 2010)

Valence state identification of individual atoms

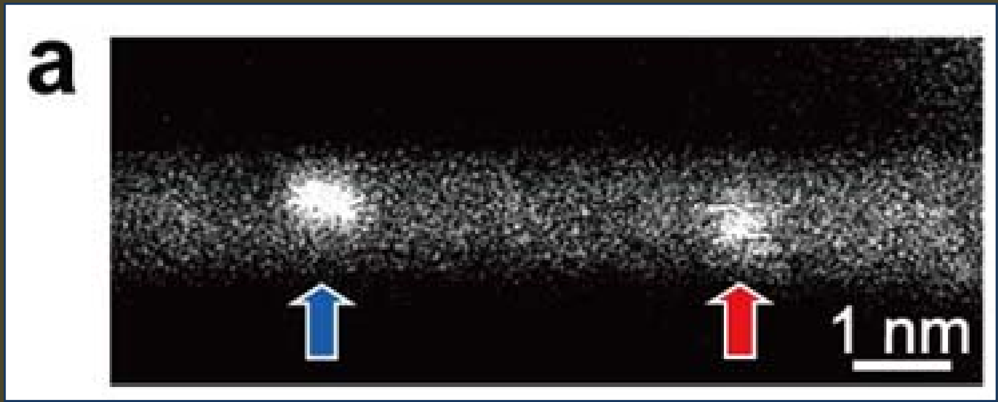

La^{3+} Ce^{3+}

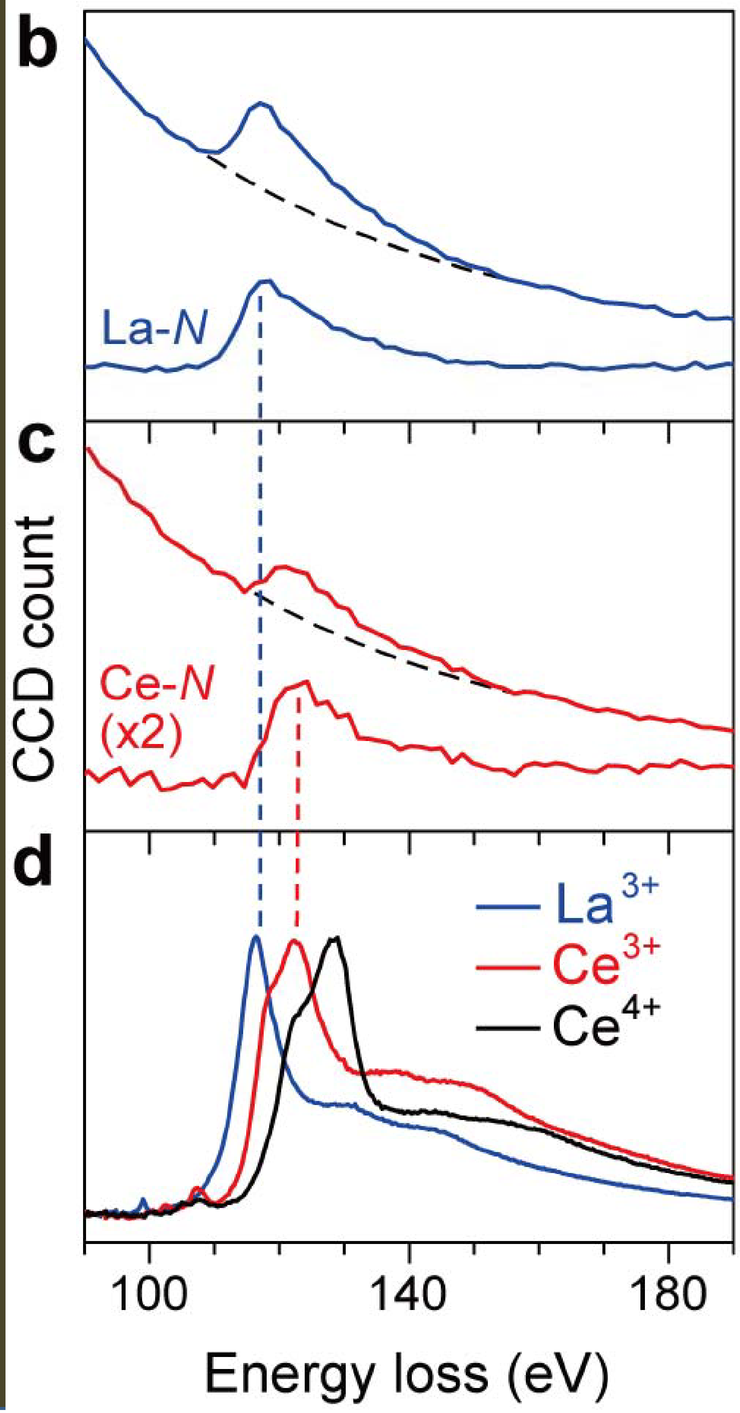

La^{3+} in $LaCl_3$
Ce^{3+} in $CeCl_3$
Ce^{4+} in CeO_2

Courtesy K. Suenaga (AIST, Tsukuba, 2010)

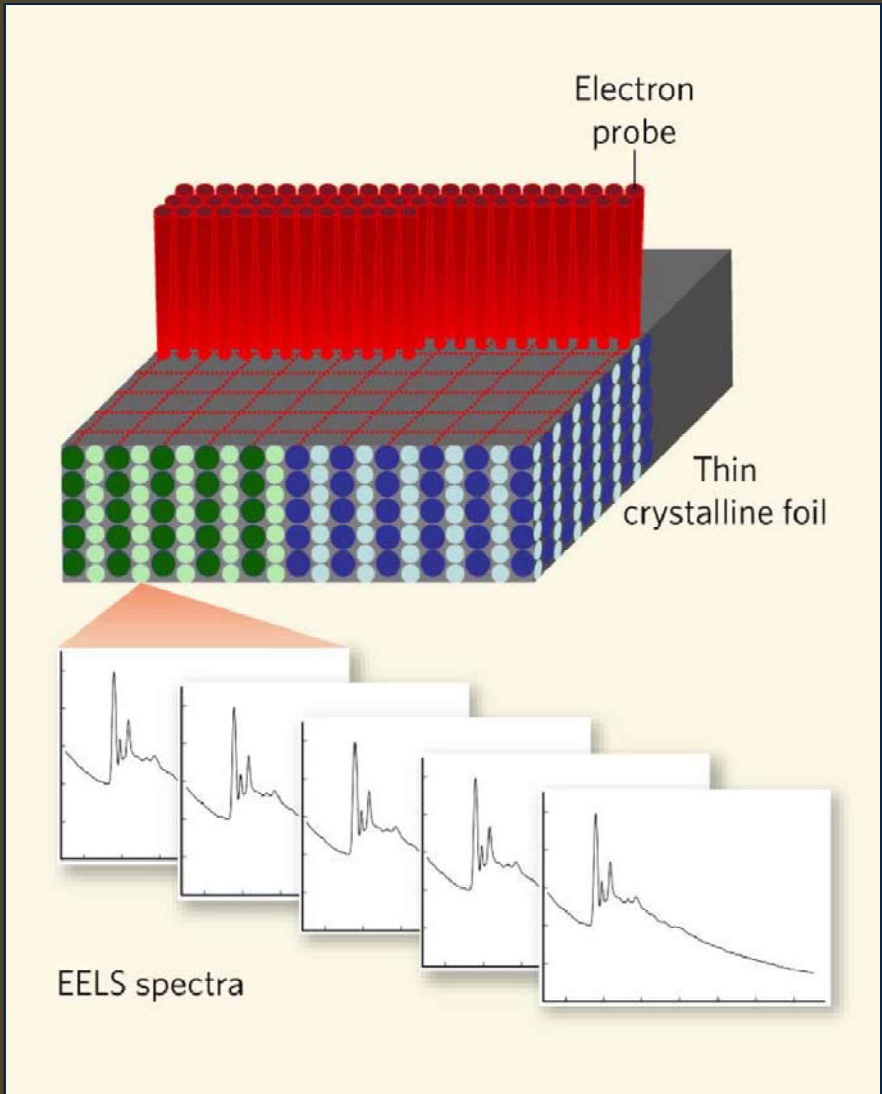

EELS spectrum-imaging across interfaces

See C. Colliex, Nature N&V (2007)

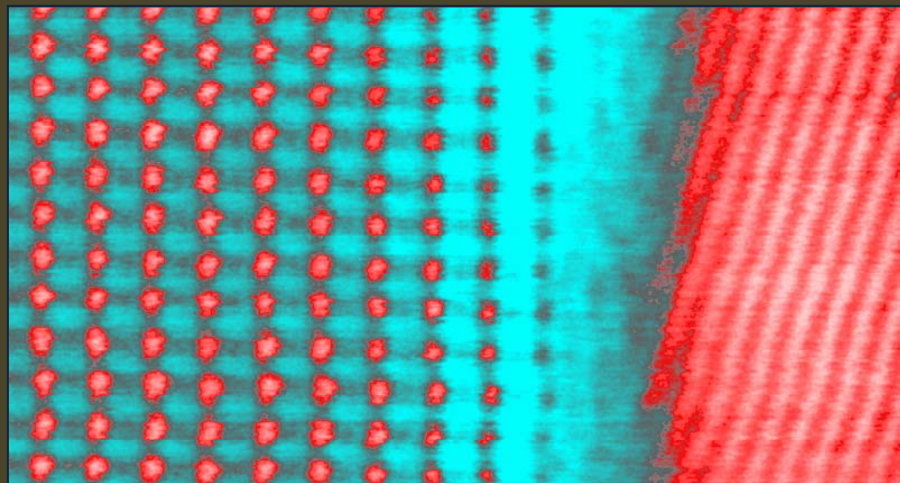

HAADF micrograph

Elemental maps recorded with NION UltraSTEM at Orsay (courtesy Laura Bocher, 2011)

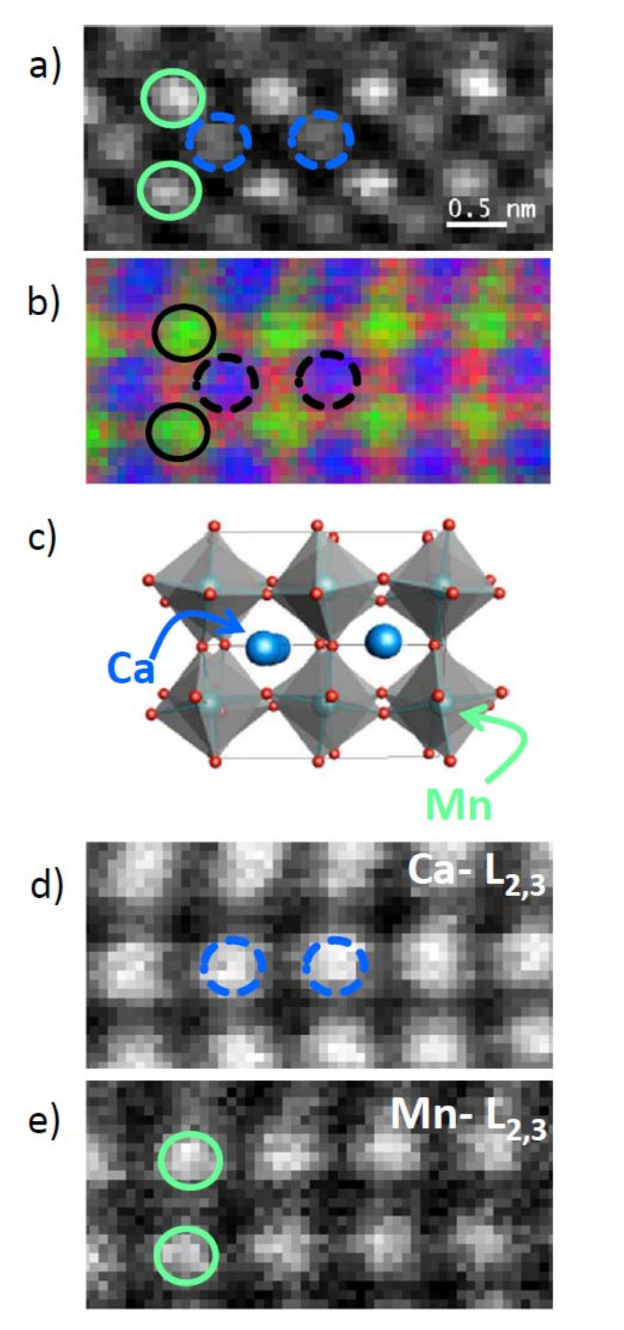

a) Atomically-resolved STEM-HAADF of $CaMn_{0.92}Nb_{0.08}O_3$ perovskite-type oxide oriented along the pseudocubic [100] zone axis, b) the false color reconstructed elemental map combining the O-*K* (red), Ca-$L_{2,3}$ (blue) and Mn-$L_{2,3}$ (green) maps, respectively, c) the corresponding structural model of the orthorhombic perovskite-type phase, d) and e) the extracted elemental map of the Ca-$L_{2,3}$ and Mn-$L_{2,3}$ edges, respectively. The acquired EELS spectra were reconstructured applying the principal component analysis method after background subtraction using a power-law fit. Blue, green, and red circles correspond to the positions of Ca, Mn, and O atoms, respectively.

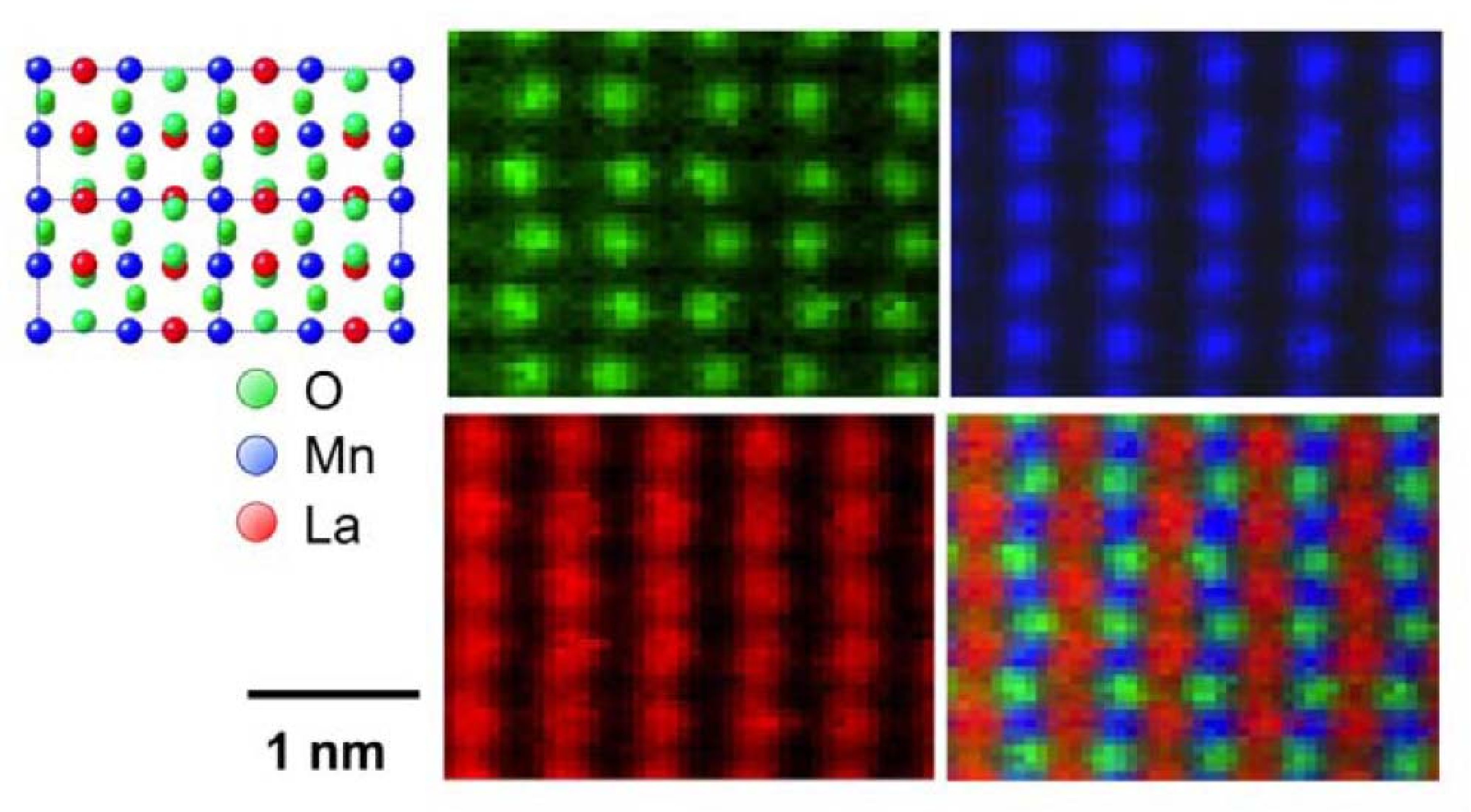

Spectroscopic imaging of LMO down the pseudocubic <110> axis. The sketch shows the projected structure of LMO down this direction. In green, the O K edge image; in blue the simultaneously acquired Mn L2,3 image and in red the La M4,5 image. The RGB overlay of the three elemental maps is also shown.
From M. Varela et al. to be published in MRS bulletin 01/2012

Atomic-Scale Chemical Imaging of Composition and Bonding by Aberration-Corrected Microscopy

D. A. Muller,[1,2]* L. Fitting Kourkoutis,[1] M. Murfitt,[3] J. H. Song,[4,5] H. Y. Hwang,[5,6] J. Silcox,[1,2] N. Dellby,[3] O. L. Krivanek[3]

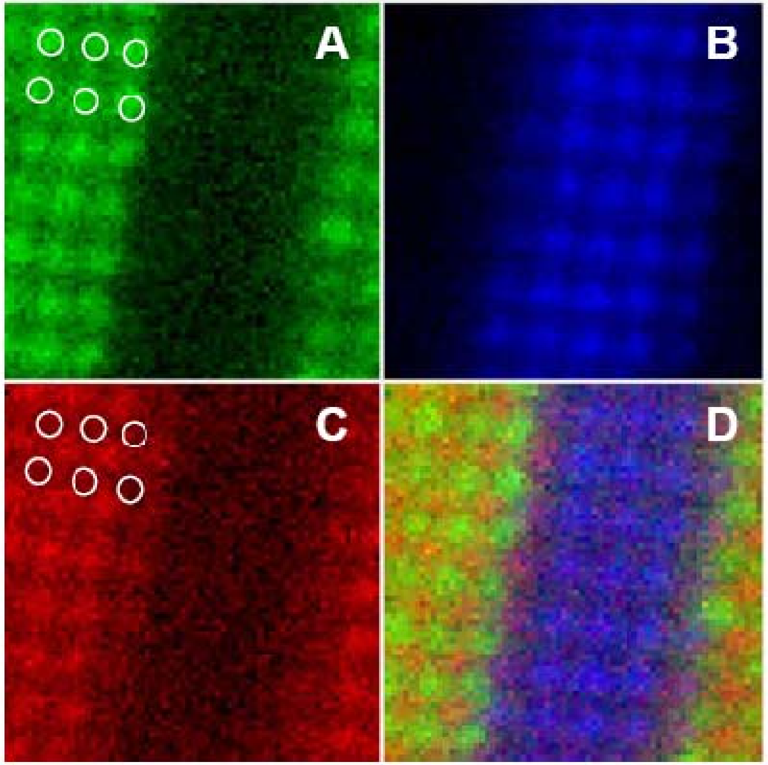

Fig. 1. Spectroscopic imaging of a $La_{0.7}Sr_{0.3}MnO_3$/$SrTiO_3$ multilayer, showing the different chemical sublattices in a 64 × 64 pixel spectrum image extracted from 650 eV–wide electron energy-loss spectra recorded at each pixel. (**A**) La M edge; (**B**) Ti L edge; (**C**) Mn L edge; (**D**) red-green-blue false-color image obtained by combining the rescaled Mn, La, and Ti images. Each of the primary color maps is rescaled to include all data points within two standard deviations of the image mean. Note the lines of purple at the interface in (D), which indicate Mn-Ti intermixing on the B-site sublattice. The white circles indicate the position of the La columns, showing that the Mn lattice is offset. Live acquisition time for the 64 × 64 spectrum image was ~30 s; field of view, 3.1 nm.

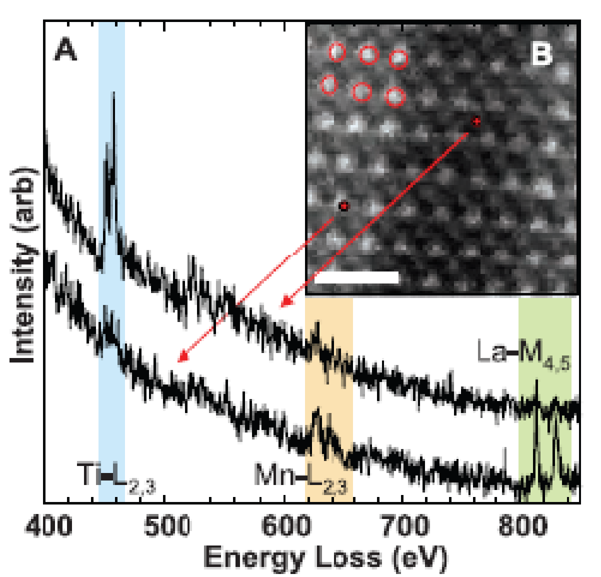

Fig. 2. (**A**) Individual EELS spectra from the series shown in Fig. 1. (**B**) The simultaneously recorded annular dark-field (ADF) image. The large red circles show that the La signal from Fig. 1A is correctly peaked where the ADF scattering is strongest. The small red dots indicate the spatial locations from which the EELS spectra were selected. Scale bar, 1 nm.

D. Muller et al. Science 319 (2008) 1073)

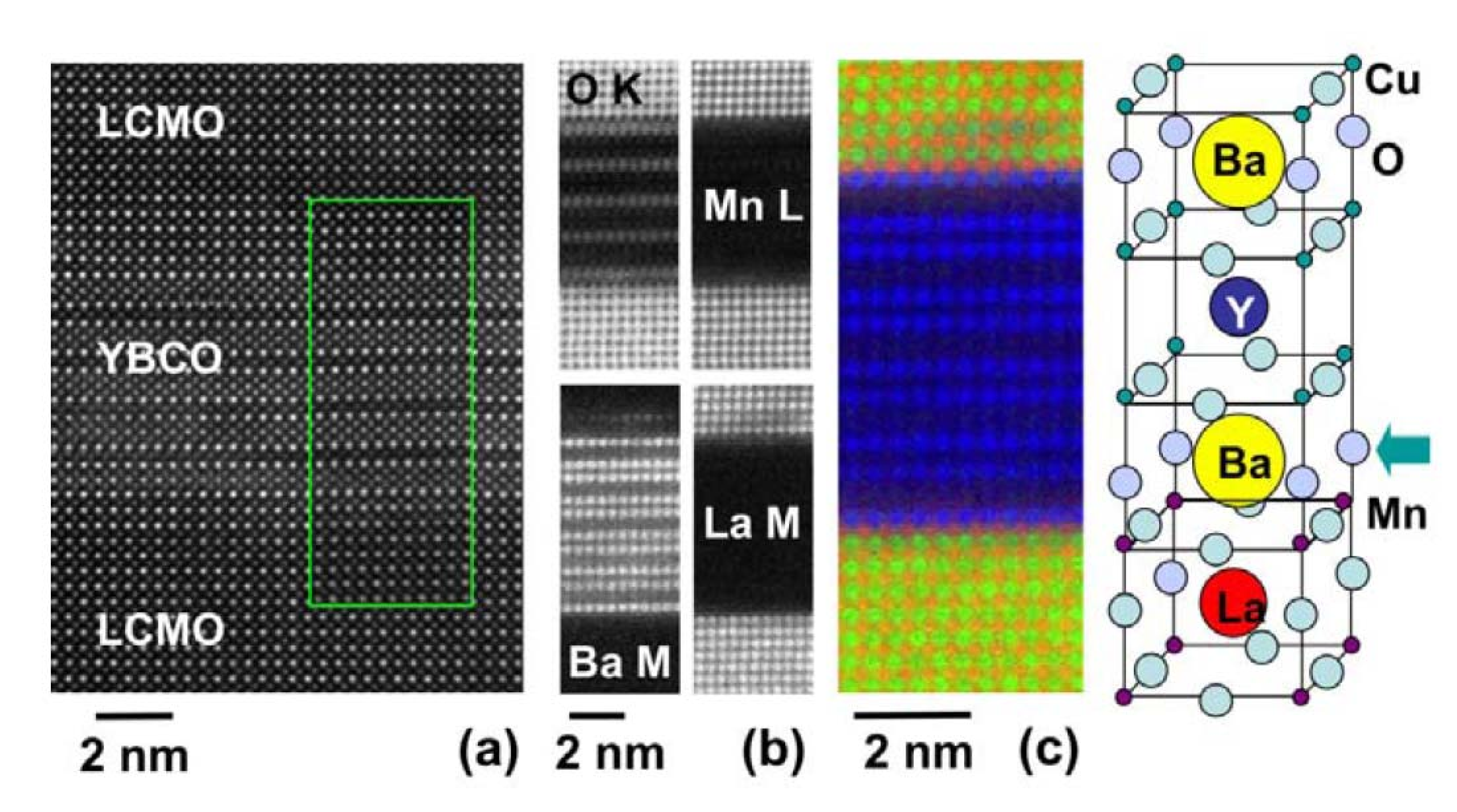

High resolution Z-contrast image of a LCMO/YBCO/LCMO heterostructure. The inset marks the region where an EELS spectrum image was acquired, along with the simultaneous ADF signal. (b) O K, Mn L2,3, Ba M4,5 and La M4,5 atomic resolution images. (c) RGB overlay of the Mn (red), La (green) and Ba (blue) images in (b). The sketch shows the interface structure.
From M. Varela et al. to be published in MRS bulletin 01/2012

Ferroelectric control of spin polarization (Tunnel ElectroMagneto Resistance – TEMR)

→ tunnel junctions with ferromagnetic electrodes for large nonvolatile control of carrier spin polarization by switching ferroelectric polarization

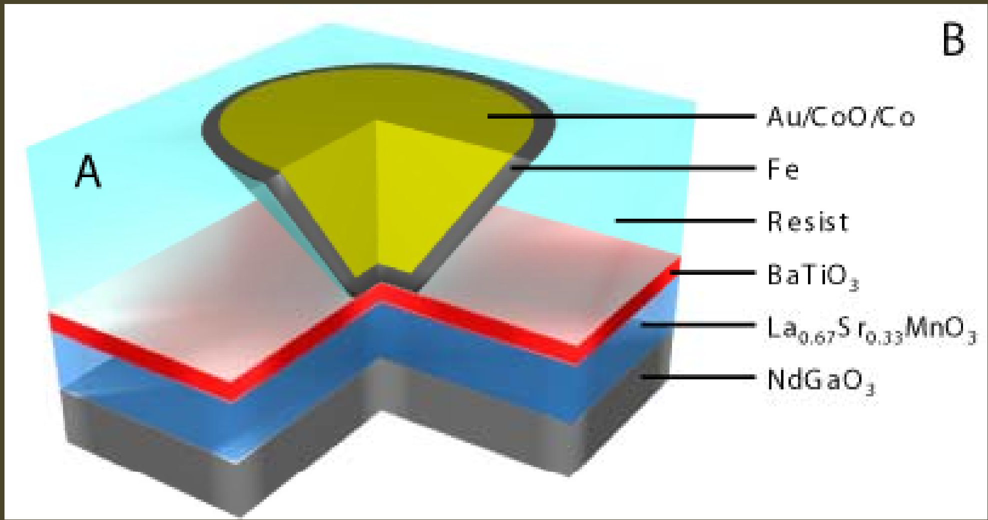

- Fe electrode
- ultrathin BTO ferroelectric
- half-metallic LSMO as spin detector
- NGO: substrate

Information provided from STEM/EELS analyses

* Structural quality of the film growth and the interfacial area

* Termination planes at the interfaces

* Oxidation states of the TM at the atomic scale

In order to understand the electromagnetic coupling at the FE/FM interface

Garcia V. *et al.* Science (2010)

Ferroelectric control of spin polarization

V. Garcia et al (Thales/CNRS Palaiseau, LPS Orsay, U. Cambridge)

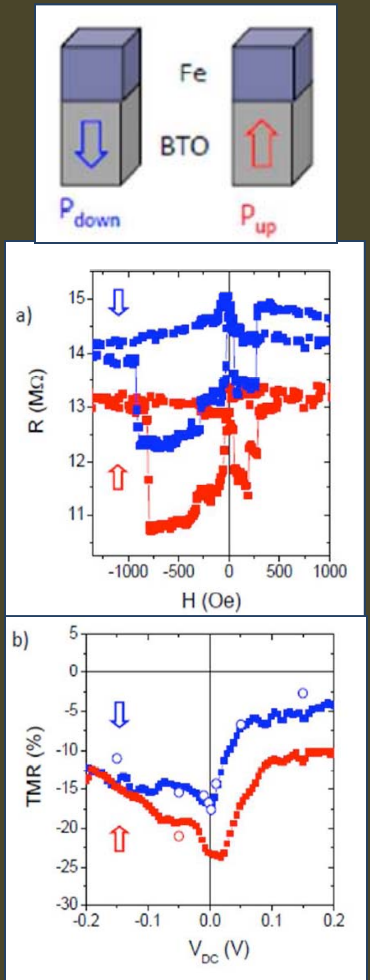

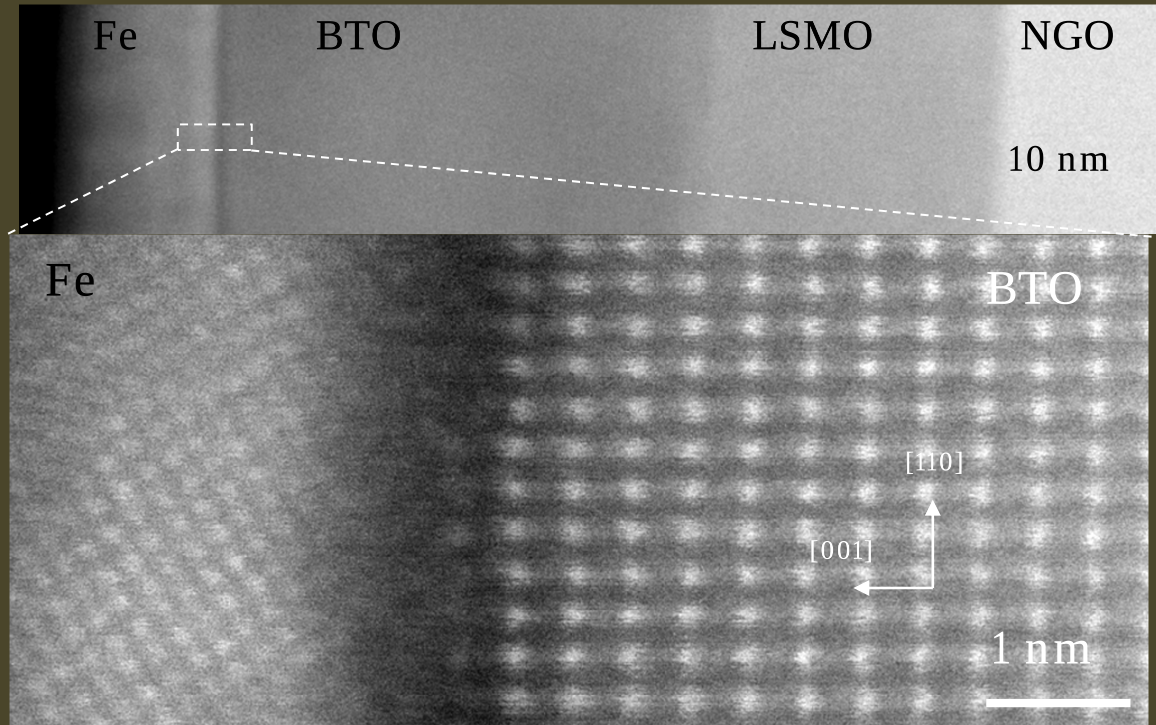

TMR (H) measured for reversed bias polarities on the ferroelectric junction

USTEM data courtesy A. Gloter & L. Bocher
L. Bocher et al. submitted (2011)

$BaTiO_3$/Fe interface

i) one possible structure model model
ii) image simulation
iii) and iv) HAADF experimental images
iv) elemental profiles

Courtesy L. Bocher & A. Gloter
JOM 62 (12/2010) 53-57

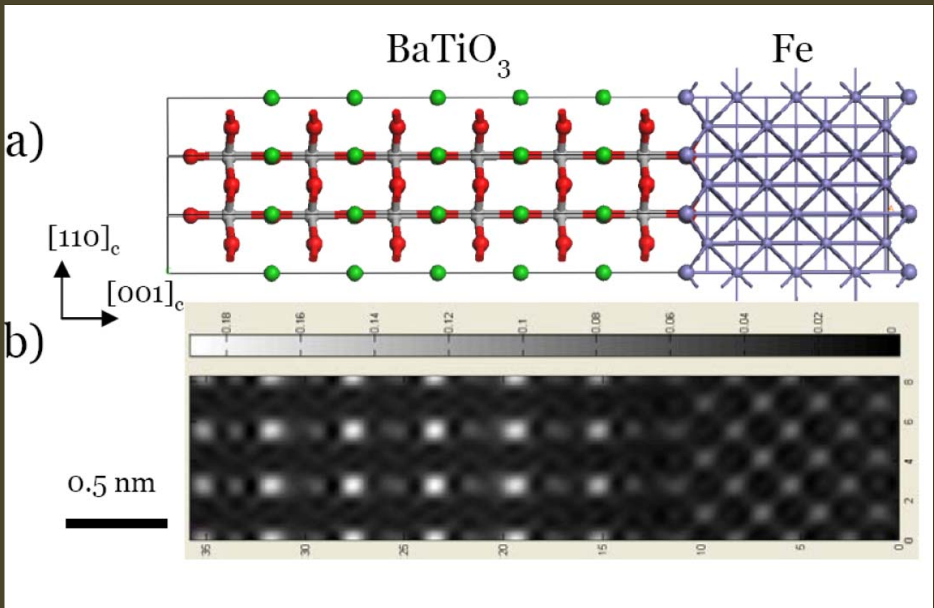

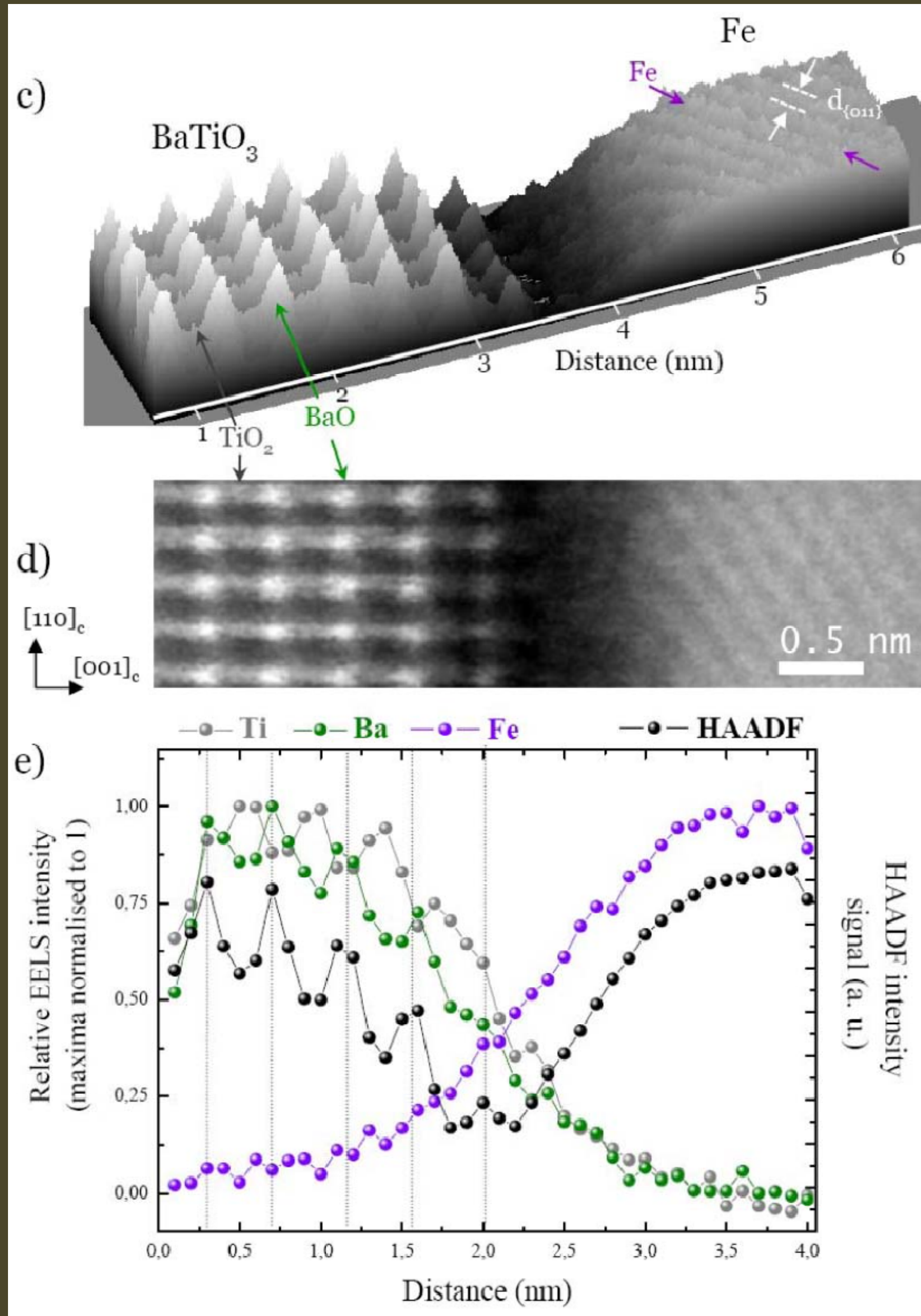

STEM imaging the interface BTO-Fe

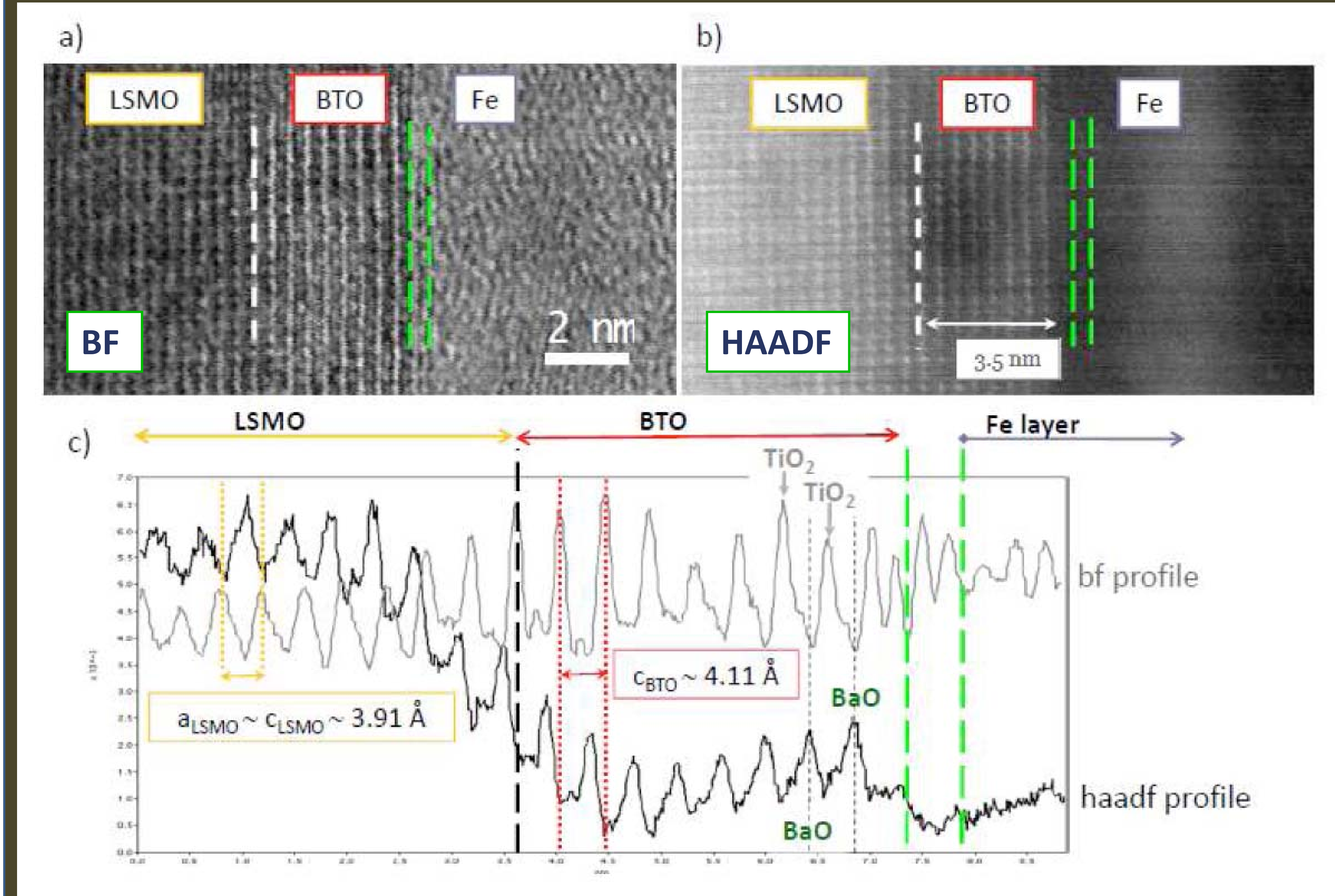

Atomic structure at the interface : comparison experiment, models and simulations

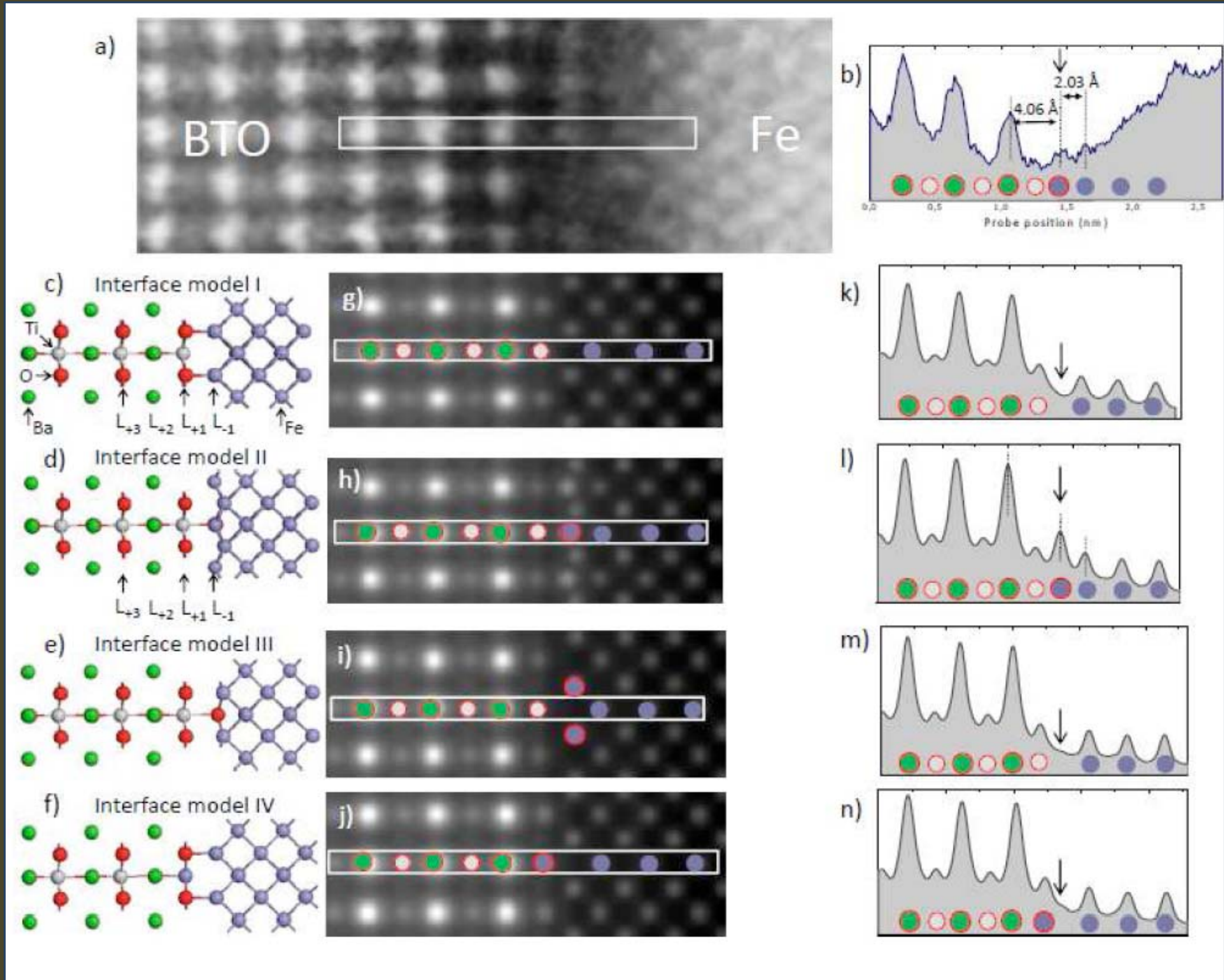

L. Bocher et al. submitted (2011)

Elemental composition and Fe EELS L_{23} fine structures across the interface

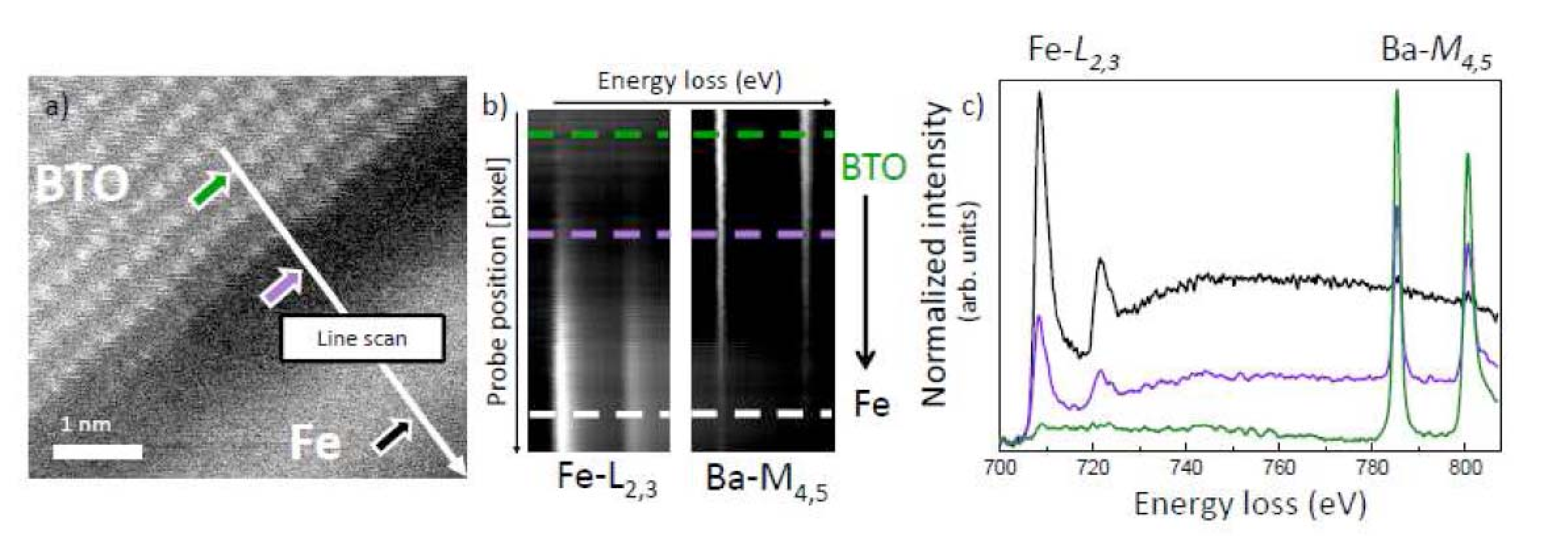

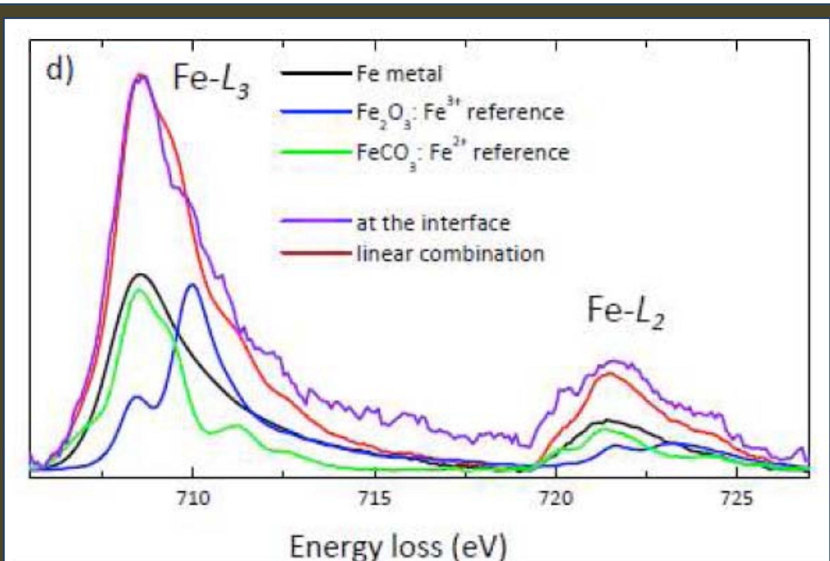

➡ **Presence of oxidized Fe (in the Fe^{++} as well as in the Fe^{+++} state) over one atomic layer at the interface**

L. Bocher et al. submitted (2011)

Modelling the interface and electronic structure calculations

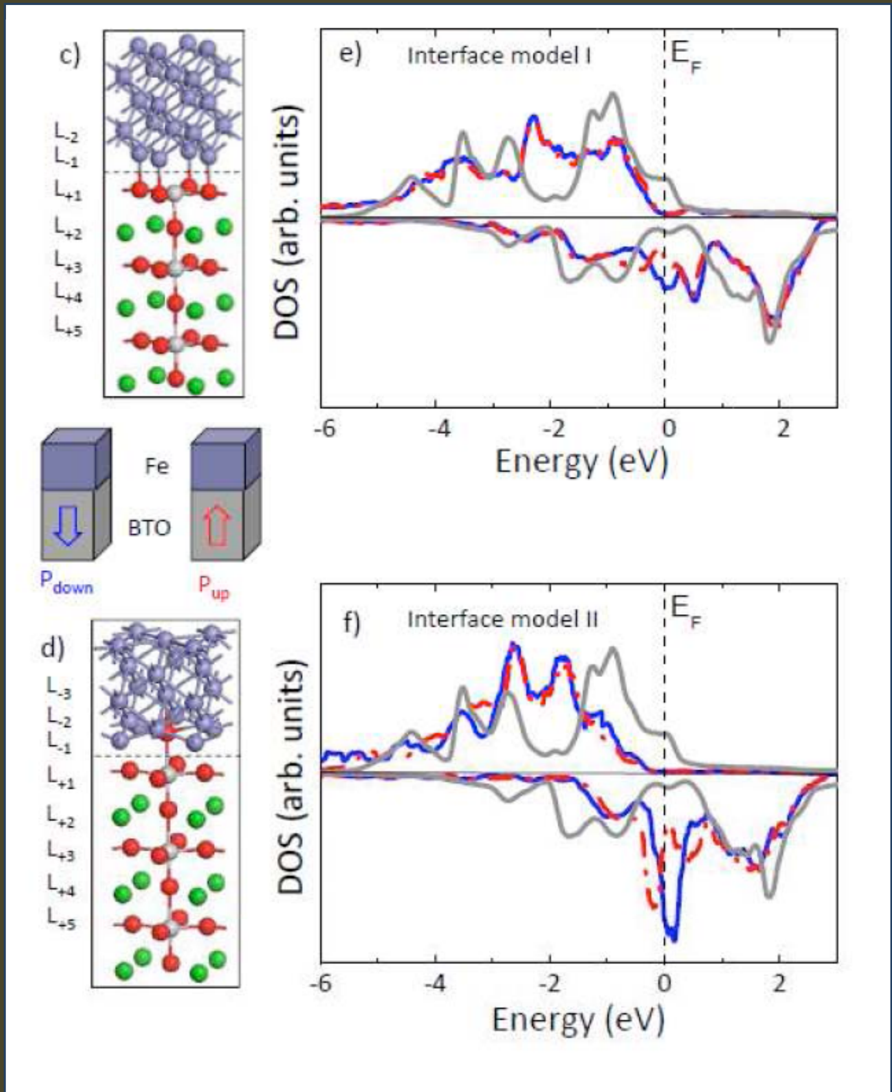

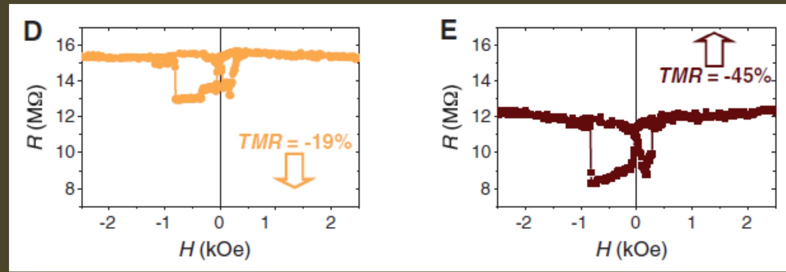

Interface model I

Interface model II

		Interface model I		Interface model II
Fe (L_{-3})	Fe [P_{up}]	2.07	Fe [P_{up}]	2.09
	Fe [P_{down}]	2.06	Fe [P_{down}]	2.05
	Δ µFe	> 0.01	Δ µFe	0.04
Fe (L_{-2})	Fe [P_{up}]	2.04	Fe [P_{up}]	2.35
	Fe [P_{down}]	2.08	Fe [P_{down}]	2.34
	D µFe	-0.04	Δ µFe	0.01
Fe (L_{-1})	Fe [P_{up}]	2.12	Fe [P_{up}]	2.85
	Fe [P_{down}]	2.31	Fe [P_{down}]	2.76
	Δ µFe	-0.19	Δ µFe	0.09

DFT calculations of the spin polarisation

L. Bocher et al. submitted (2011)

Trends of the accessible performance in terms of spatial and spectral resolution (updated in 2010)

Must be accompanied with a parallel development in data processing and modelization tools (propagation of a sub-angström electron probe across a thin specimen, physics of the inelastic scattering, calculation of electron density of states…)

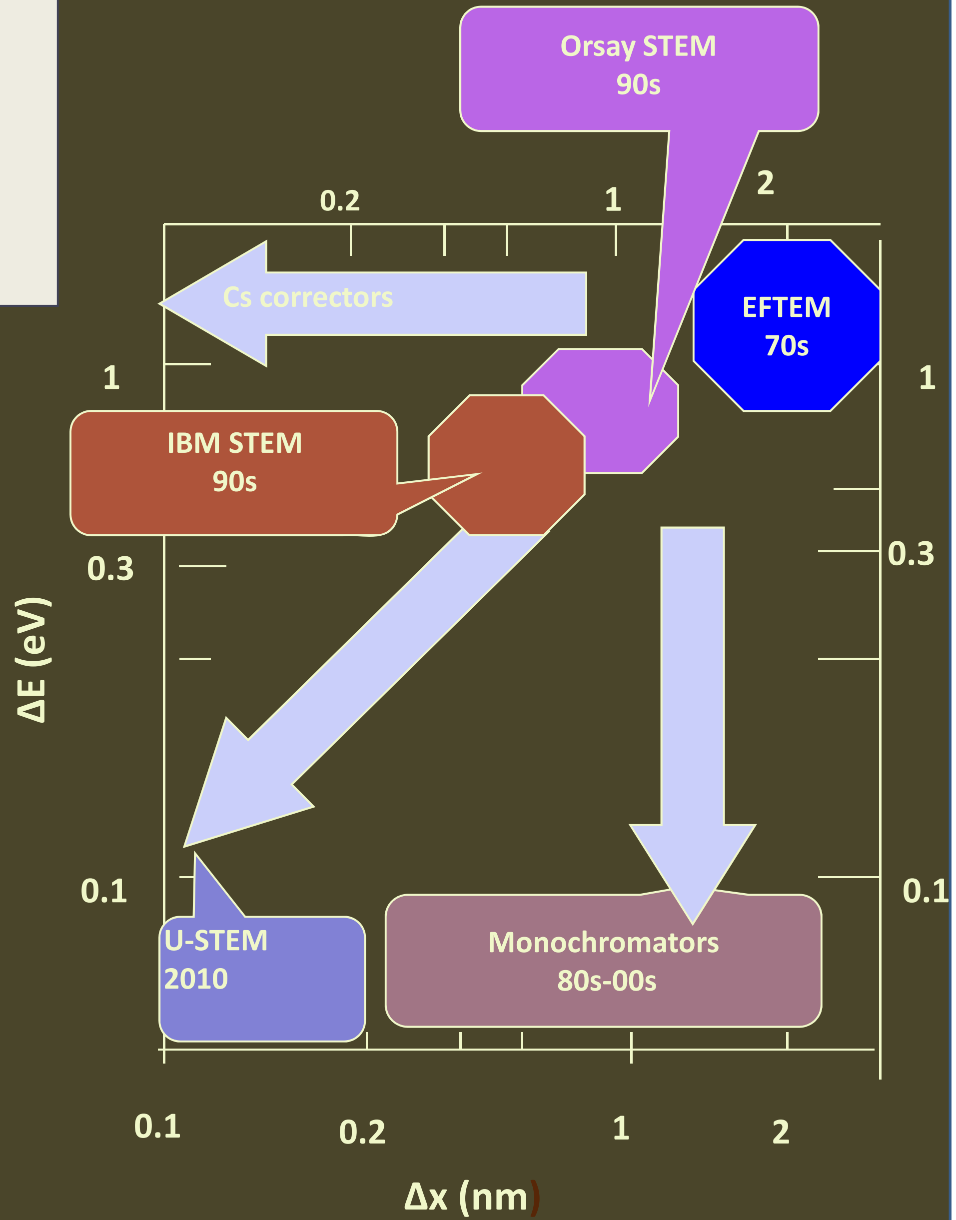

Where are we now ?

Mapping plasmons and EM fields

4D (x,y,E,t) Spectrum-imaging mode

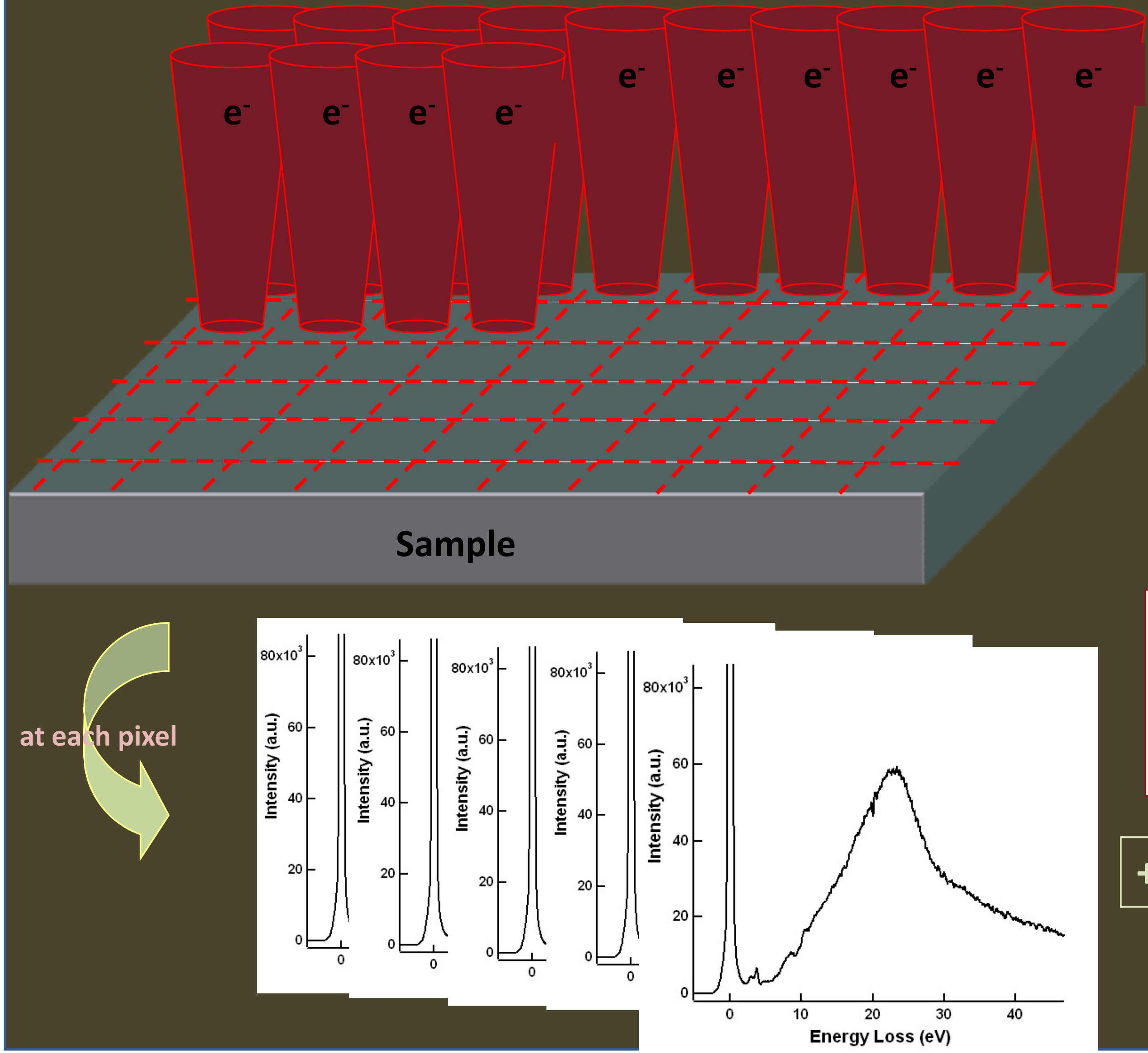

Improved energy resolution (0.2 eV)

- 50 spectra/pixel
- 3 ms/spectrum
- deconvolution

+ HAADF signal

New possibilities for studying the low energy-loss domain

Deconvolution techniques open the way to investigating nanophotonics with electrons

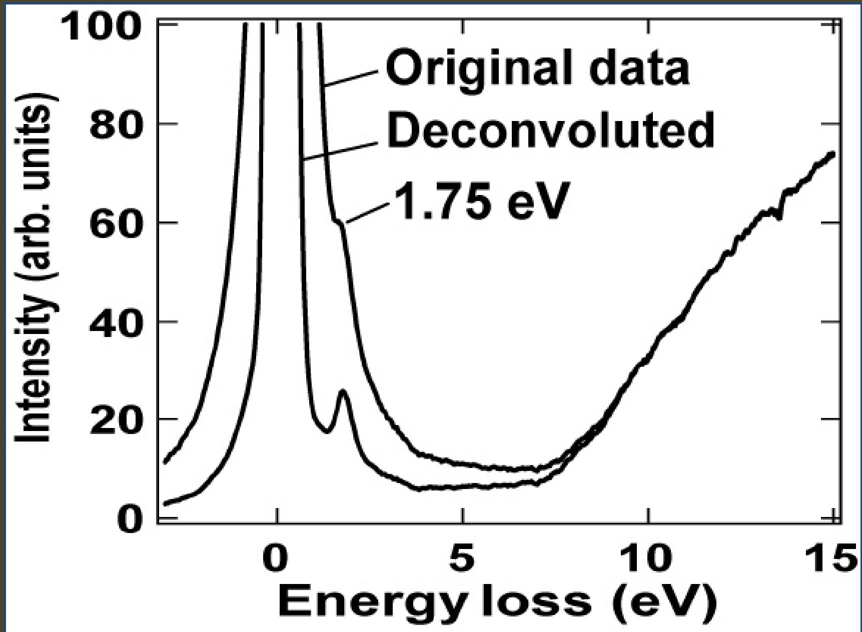

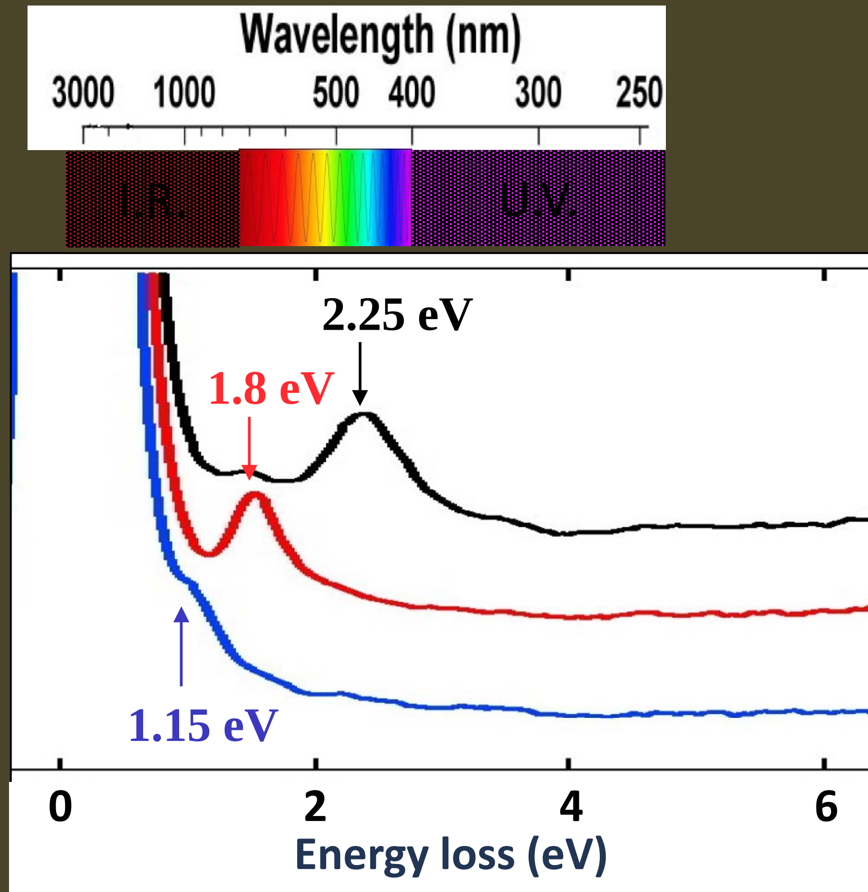

Increase in ΔE
(from 0.35 eV to 0.25 eV)

Cut-off of zero loss signal
at 0.9 eV (IR)

Higher
signal-to-background ratio

New technical possibilities (A. Gloter, A Douiri, M. Tencé)

Mapping surface plasmon resonances of triangular silver nanoprisms

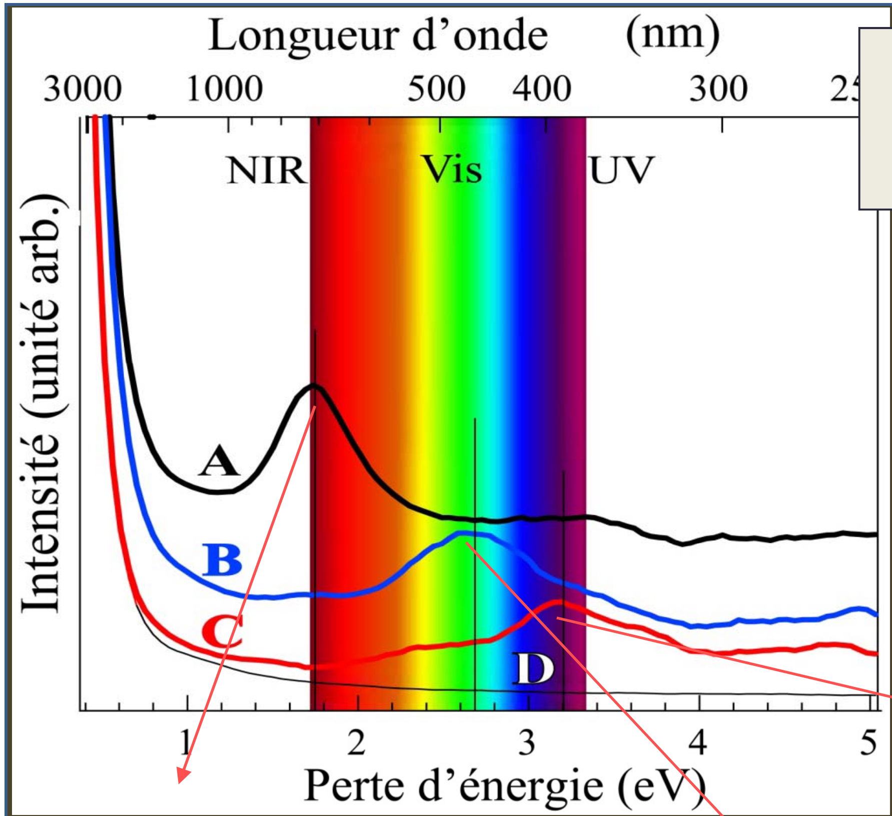

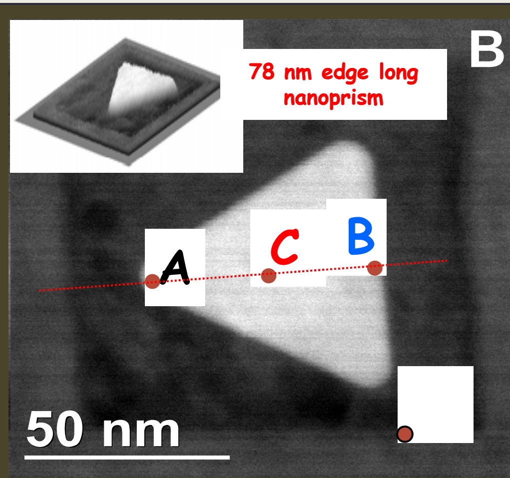

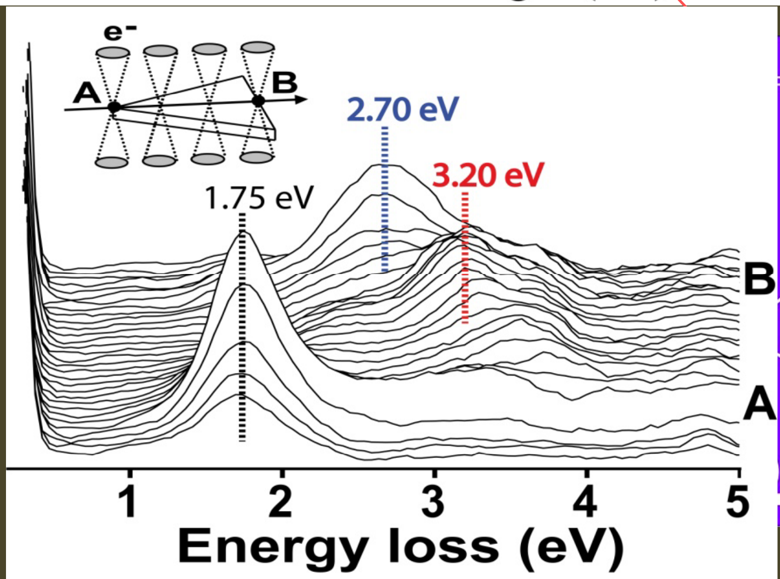

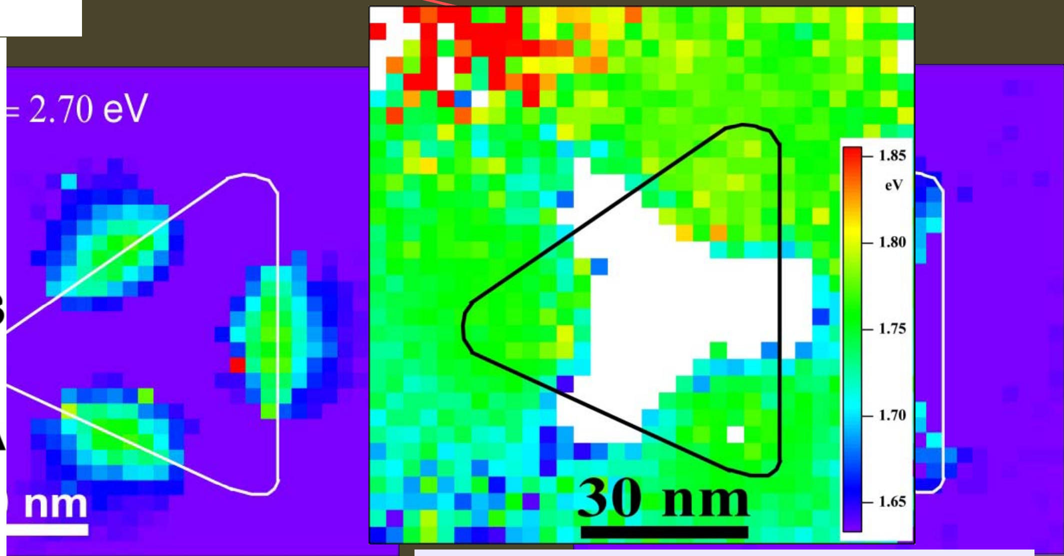

Energy map of the "tip" mode

J. Nelayah *et al.* *Nature Physics, 3, 348-353 (2007)*

EELS simulations of triangular Ag nanoprisms

(courtesy J. Garcia de Abajo, Madrid)

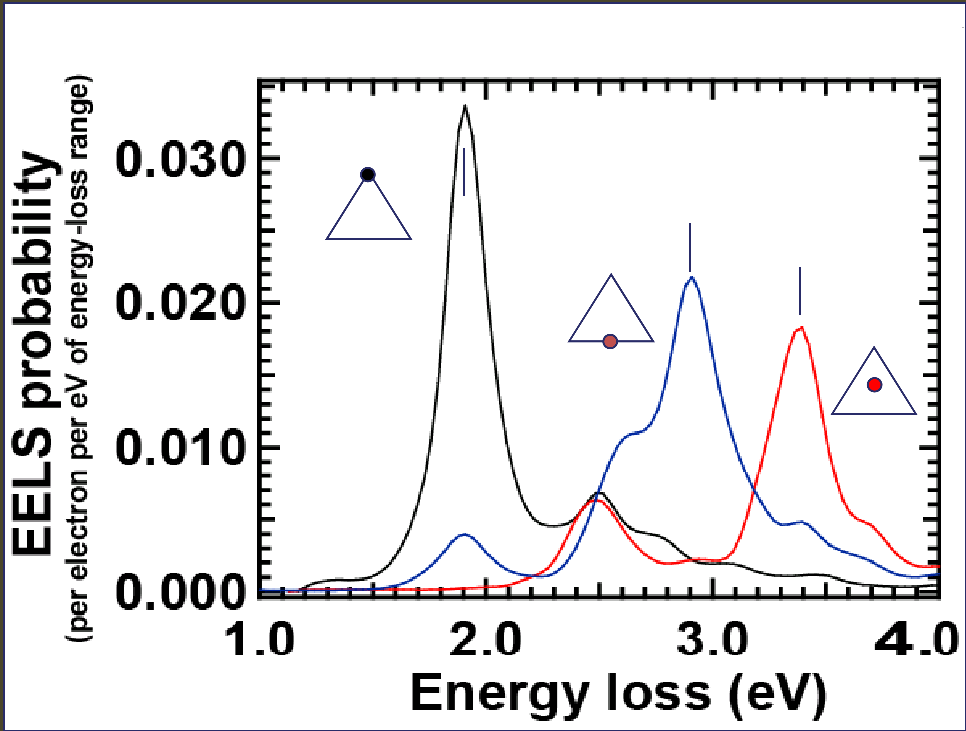

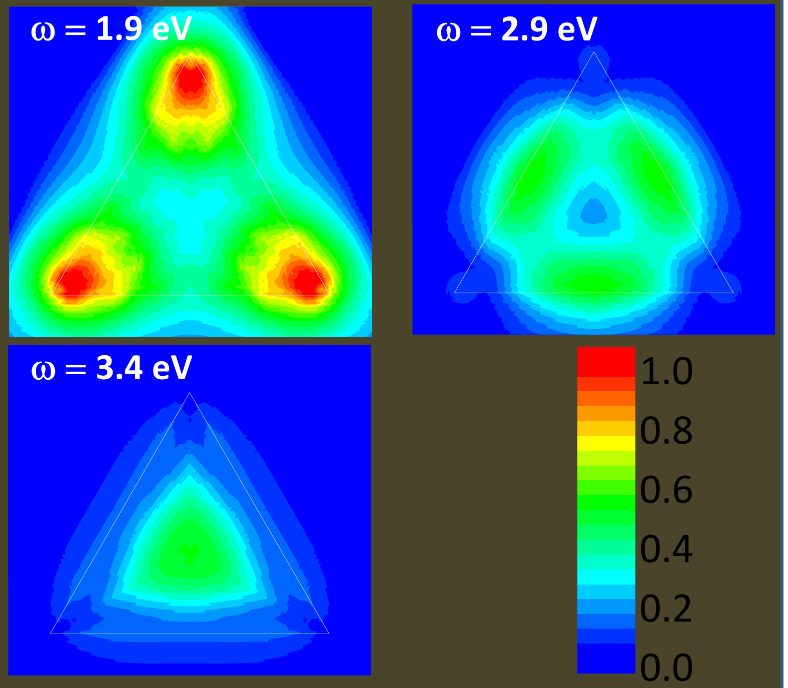

- 100 Kv electrons
- 78 nm long and 10 nm thick Ag prism

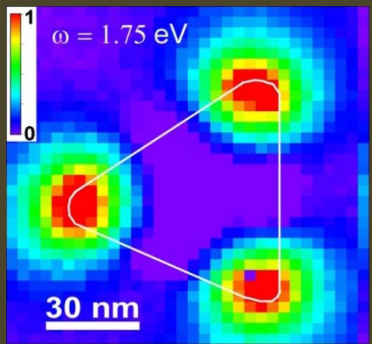

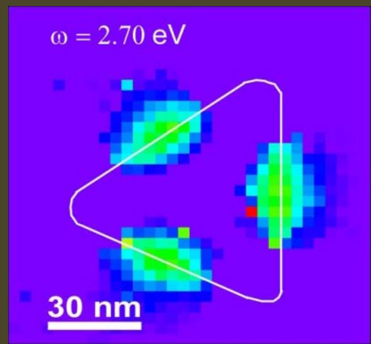

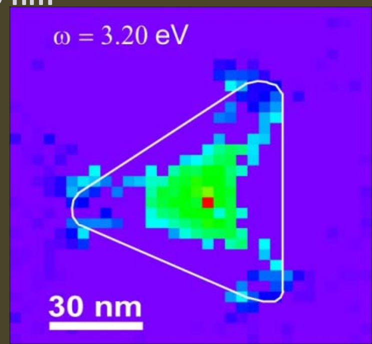

Modes in an Ag nanoantenna (aspect ratio L/r increases)

(coll. Cambridge-Stuttgart, courtesy P. Midgley)

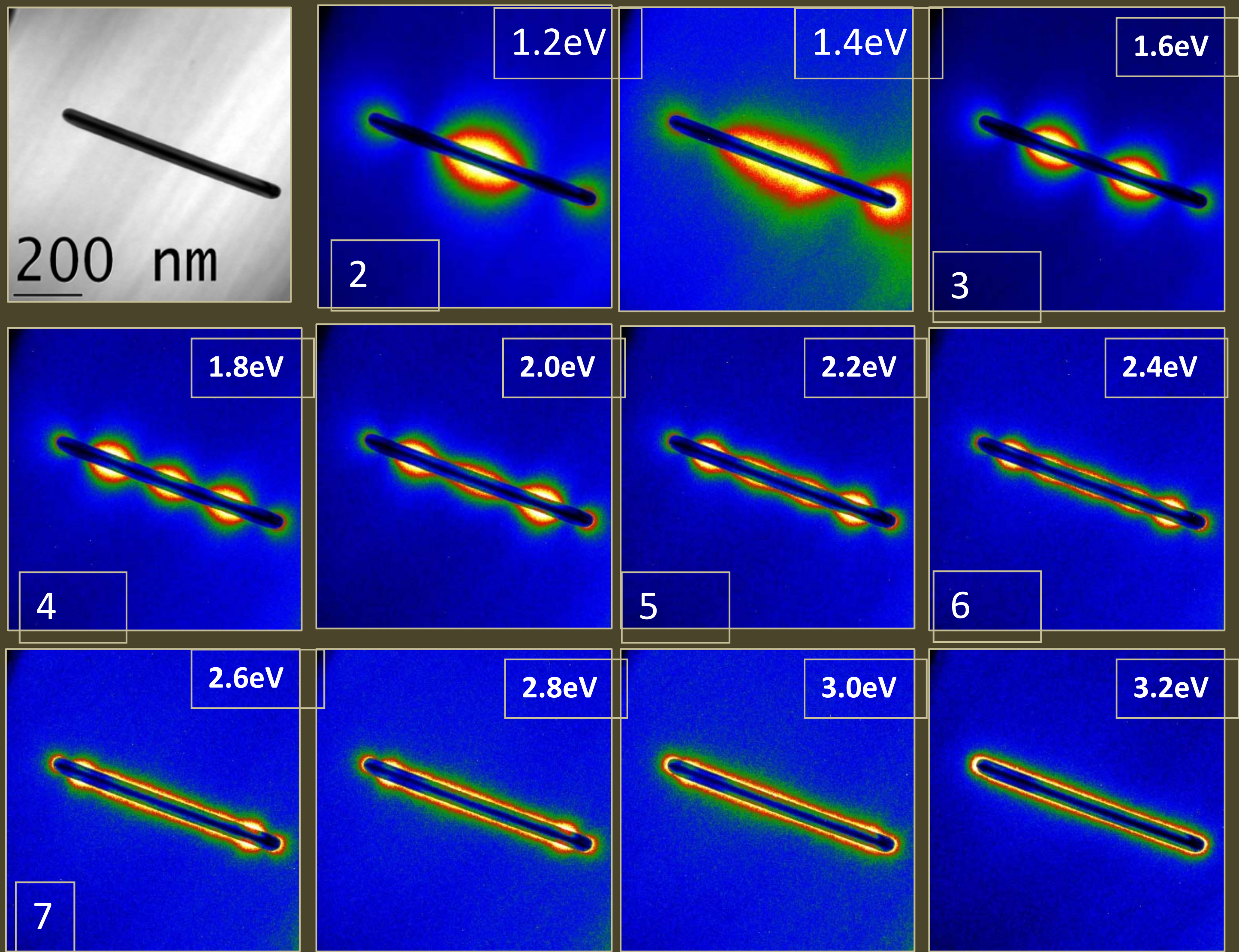

EFTEM series on SESAM machine

660 nm Ag nanorod

0.2eV slit width

Silver nanoantennas EELS (2)

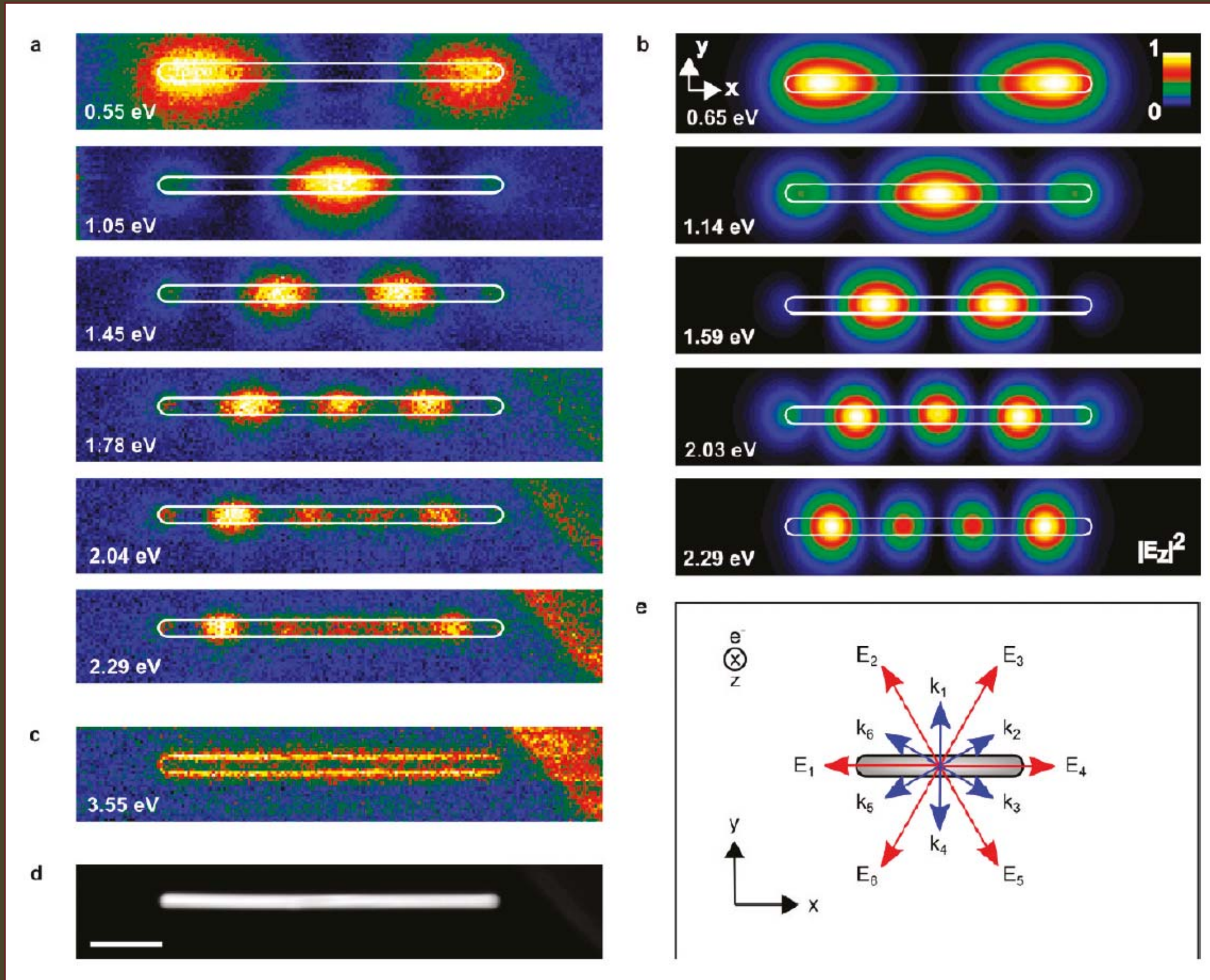

Experiments versus simulations
(DDA of $|E_z|^2$ at 60 nm above antenna)

Nano Lett 11, 1499 (2011)

When electrons and photons team up

« Multi-signal microscopy »

« When electrons and photons team up »

by F.J. Garcia de Abajo (Nature 462 (2009) 861)

8 JOURNAL OF ELECTRON MICROSCOPY, 2011

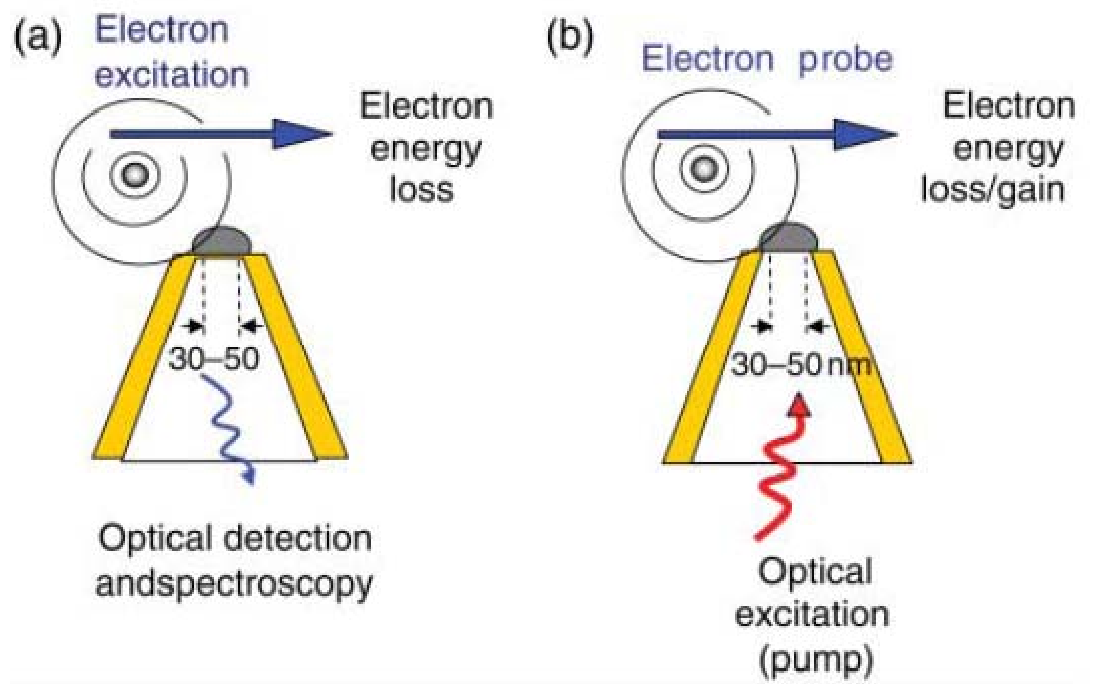

Fig. 7. Schematic description of novel multi-signal microscopies involving dual beams (photons and electrons) either as probing particles or as generated signals: one recognizes in (a) the conventional EELS (electron/electron) spectroscopy and the more original (electron /photon – either X or visible) mapping modes, and in (b) the much more innovative (photon/electron) mode corresponding to electron energy gain or electron energy loss of excited states, see text for further description (image courtesy of M. Kociak).

Light detection (inserting a parabolic mirror within the VG pole piece)

home-made cold stage + light detector (L. Zagonel+ S. Mazzucco + M. Kociak)

Monochromatic electron beam

Electron **I**nduced **R**adiation **E**mission (Cathodoluminescence)

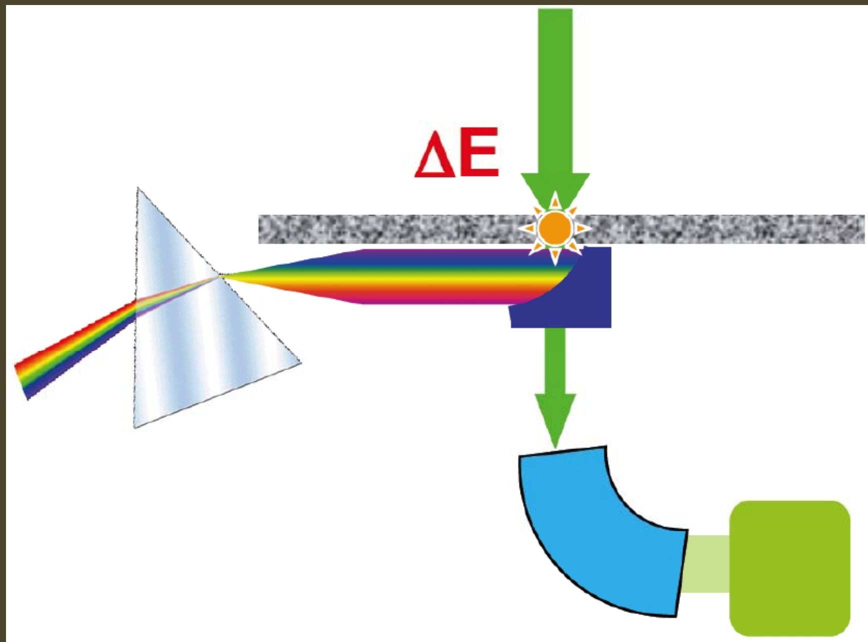

Electron Energy-Loss Spectrum

Emission by CL

Absorption by EELS

2 patents (licensing opportunities)

NANO LETTERS
dx.doi.org/10.1021/nl103549t | Nano Lett.
LETTER
pubs.acs.org/NanoLett

Nanometer Scale Spectral Imaging of Quantum Emitters in Nanowires and Its Correlation to Their Atomically Resolved Structure

Luiz Fernando Zagonel,[†] Stefano Mazzucco,[†] Marcel Tencé,[†] Katia March,[†] Romain Bernard,[†] Benoît Laslier,[†] Gwénolé Jacopin,[‡] Maria Tchernycheva,[‡] Lorenzo Rigutti,[‡] Francois H. Julien,[‡] Rudeesun Songmuang,[§] and Mathieu Kociak[*,†]

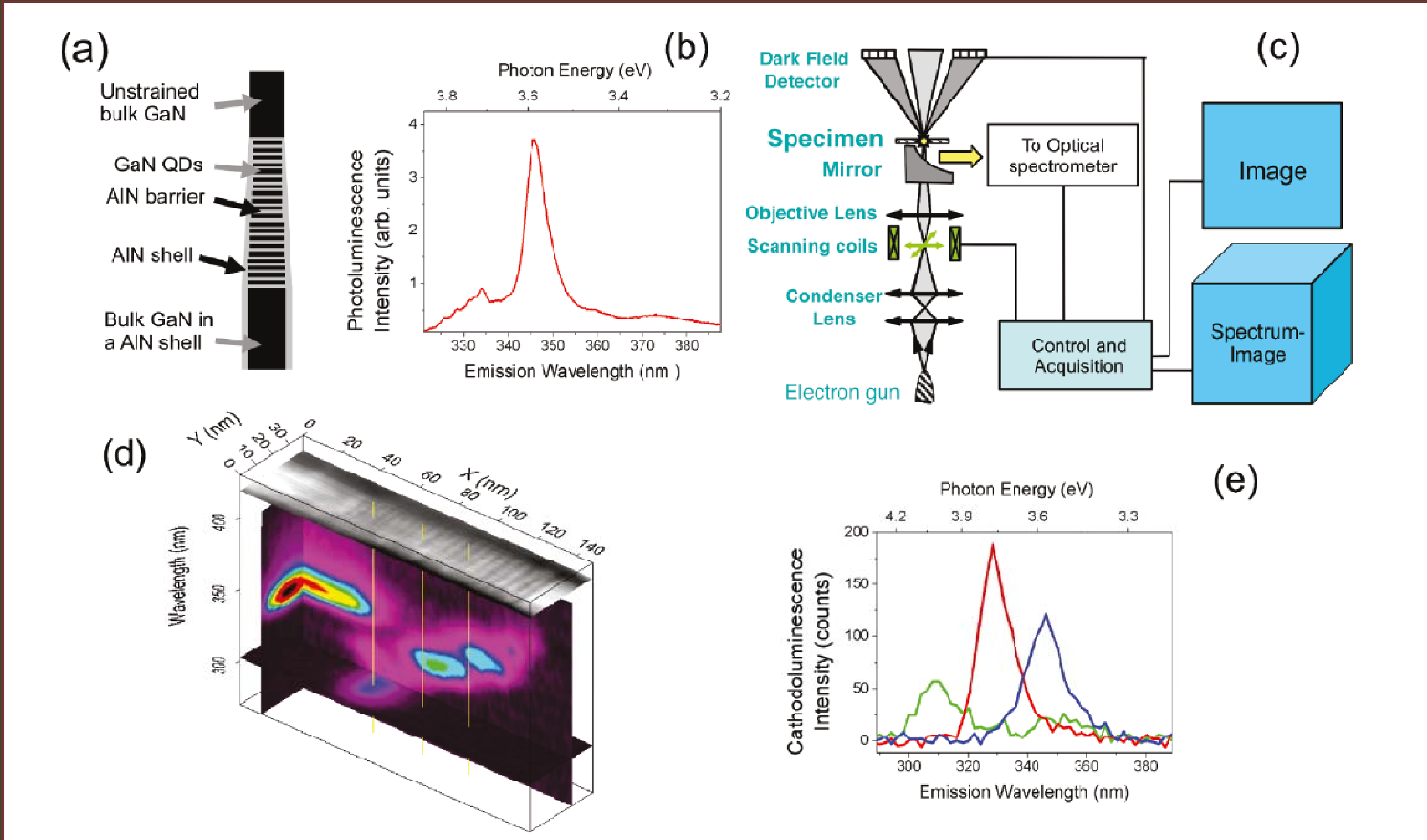

2D photon emission spectral-imaging

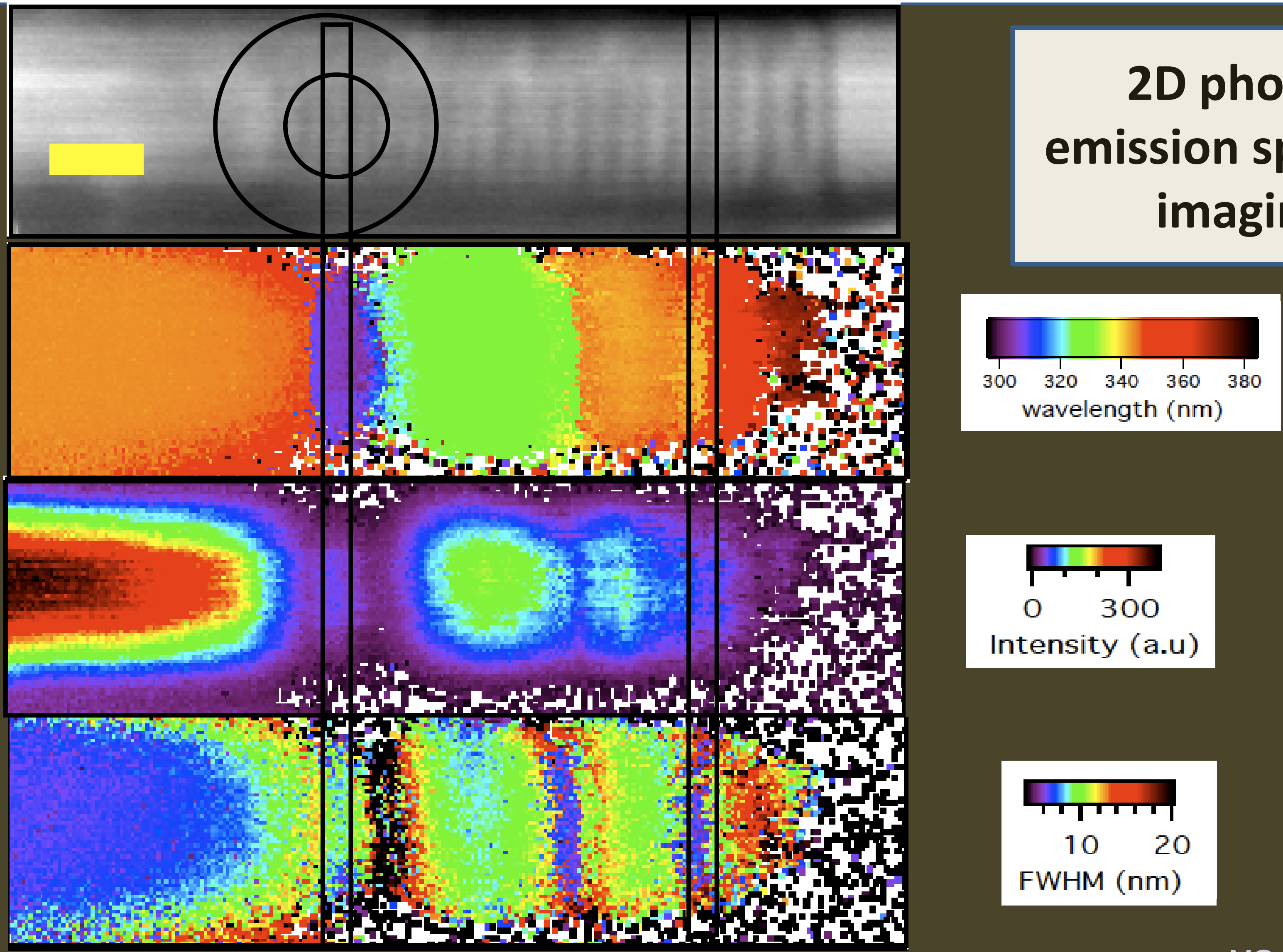

VG HB501

- Spatial sampling: 0.7 nm
- Spectral sampling: 2 nm (ca 8 meV)
- Individual QD optical properties revealed!

L. Zagonel, M. Kociak et al., NanoLetters 2011

Spectral Imaging with electrons

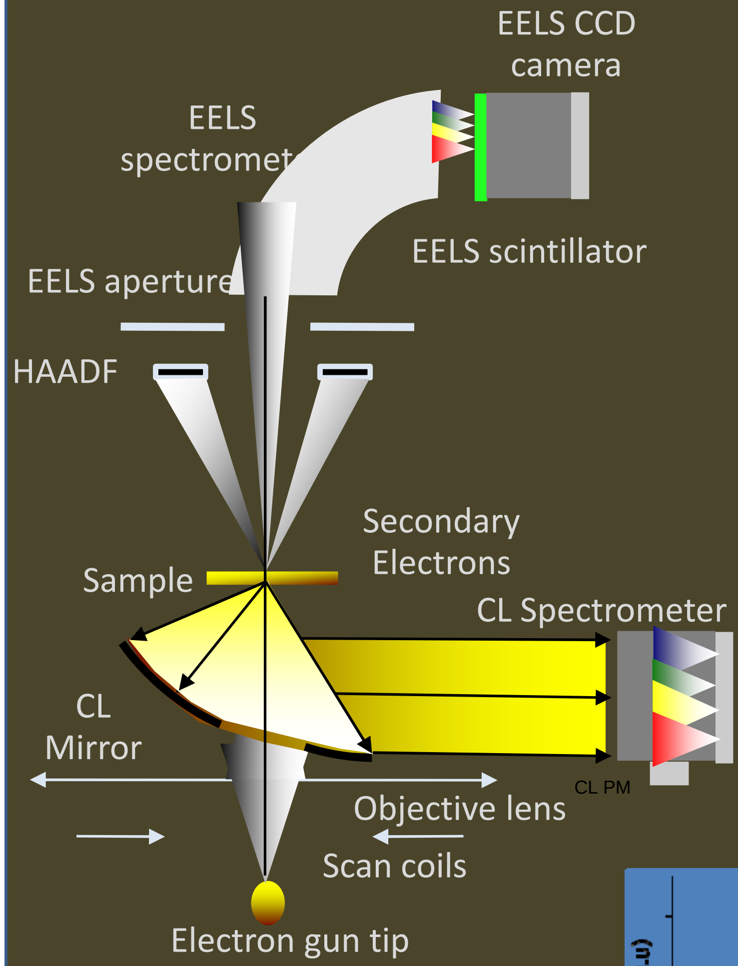

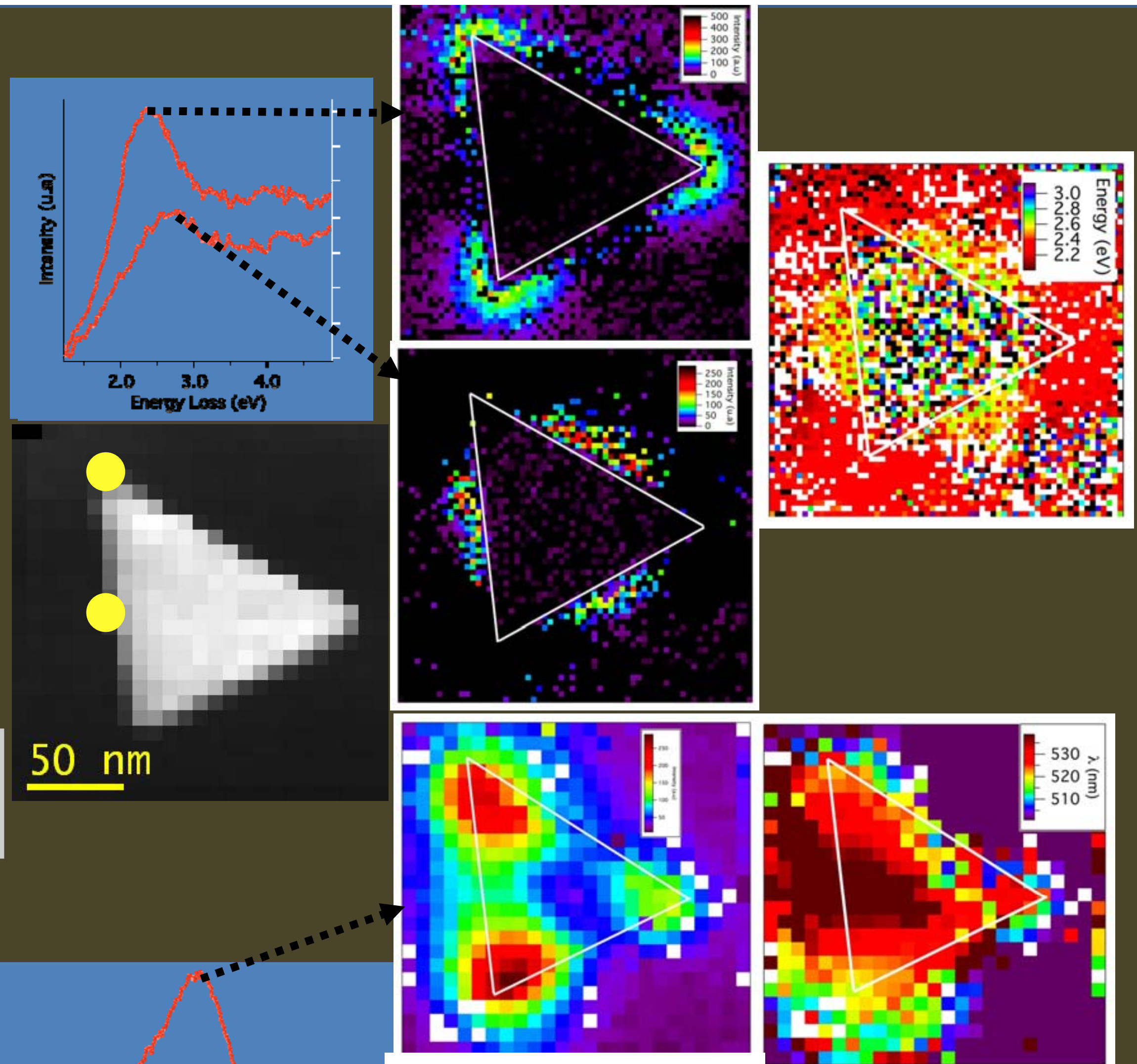

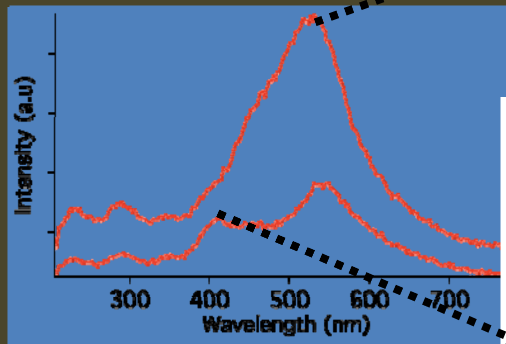

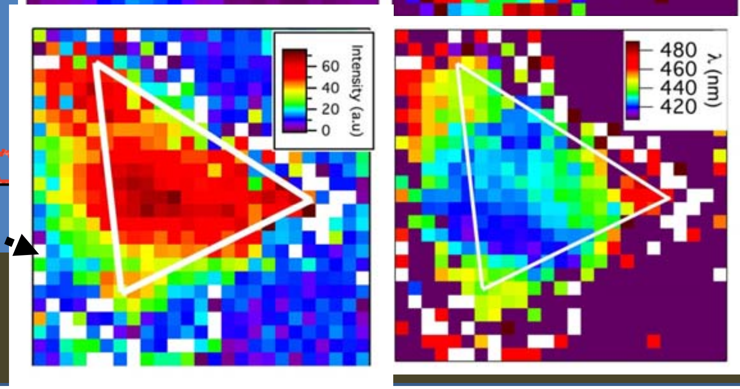

M. Kociak et al., patents pending
L. Zagonel, A. Losquin et al., unpublished,

- Absorption and emission on the same object
  - @ nm resolutions..

Absorption and Emission

multi-detection: HADF+ EELS + EIRE (CL)

first proof of principle for simultaneous **EELS/EIRE**

symmetry of the modes, modal decomposition?

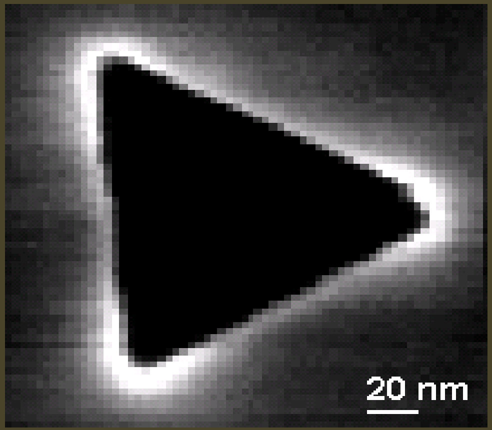

Energy 2.2 eV

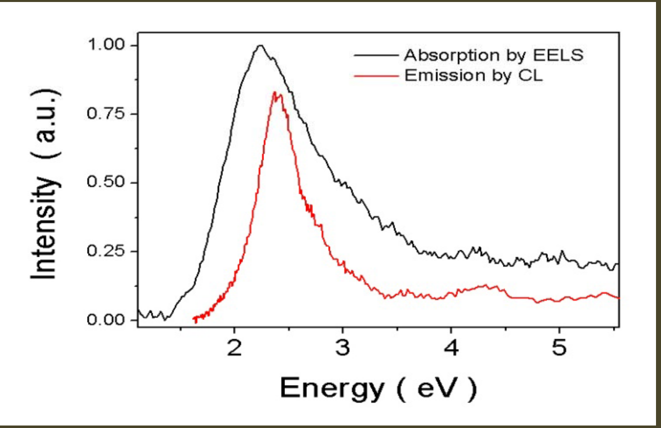

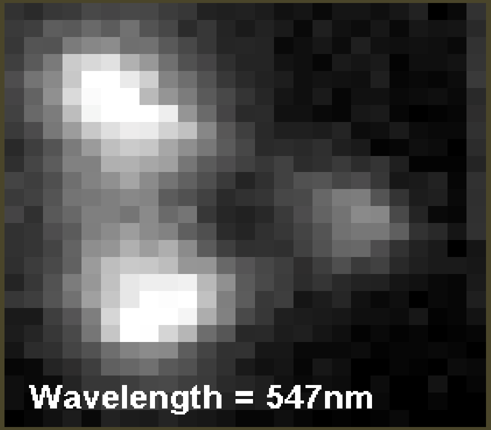

EELS
(radiative and non radiative modes)

CL
(only radiative modes)

No energy resolution limitation by the PSF detection system:
optical spectroscopy at a true nanometer scale

Photon-induced near-field electron microscopy

Brett Barwick[1], David J. Flannigan[1] & Ahmed H. Zewail[1]

Nature, 17 december 2009

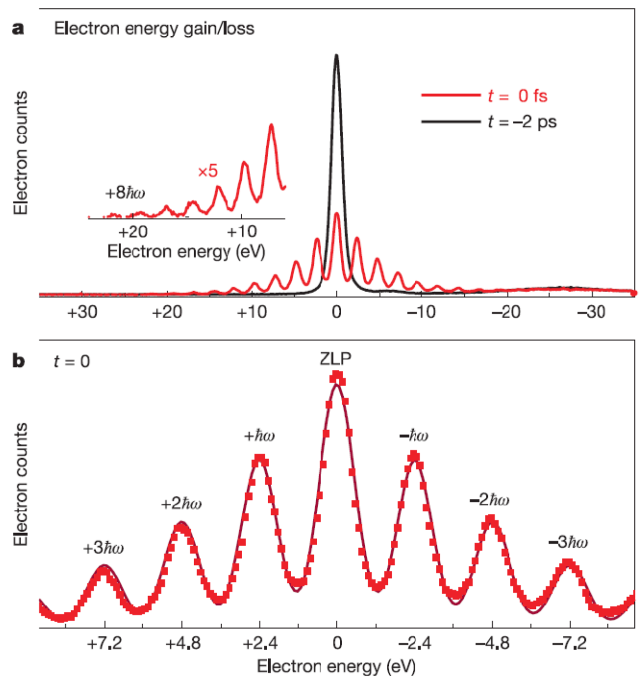

Figure 1 | Electron energy spectra of carbon nanotubes irradiated with an intense fs laser pulse at two different delay times. a, The zero-loss peak (ZLP) of the 200 keV electrons (black curve) taken when the electron packet arrives before the femtosecond pulse; in this spectrum only the plasmon peaks are present (see text). The energy spectrum at coincidence of the two pulses ($t = 0$ fs; red curve) displays the multiple quanta of photon absorption/emission. Inset, the positive energy gain region multiplied by 5 for the $t = 0$ spectrum, indicating that absorption of at least eight quanta of photon energy can be observed at maximum spatiotemporal overlap. **b**, Magnified view of the electron energy spectrum obtained at $t = 0$. The energy is given in reference to the loss/gain of photon quanta by the electrons with respect to the zero-loss energy.

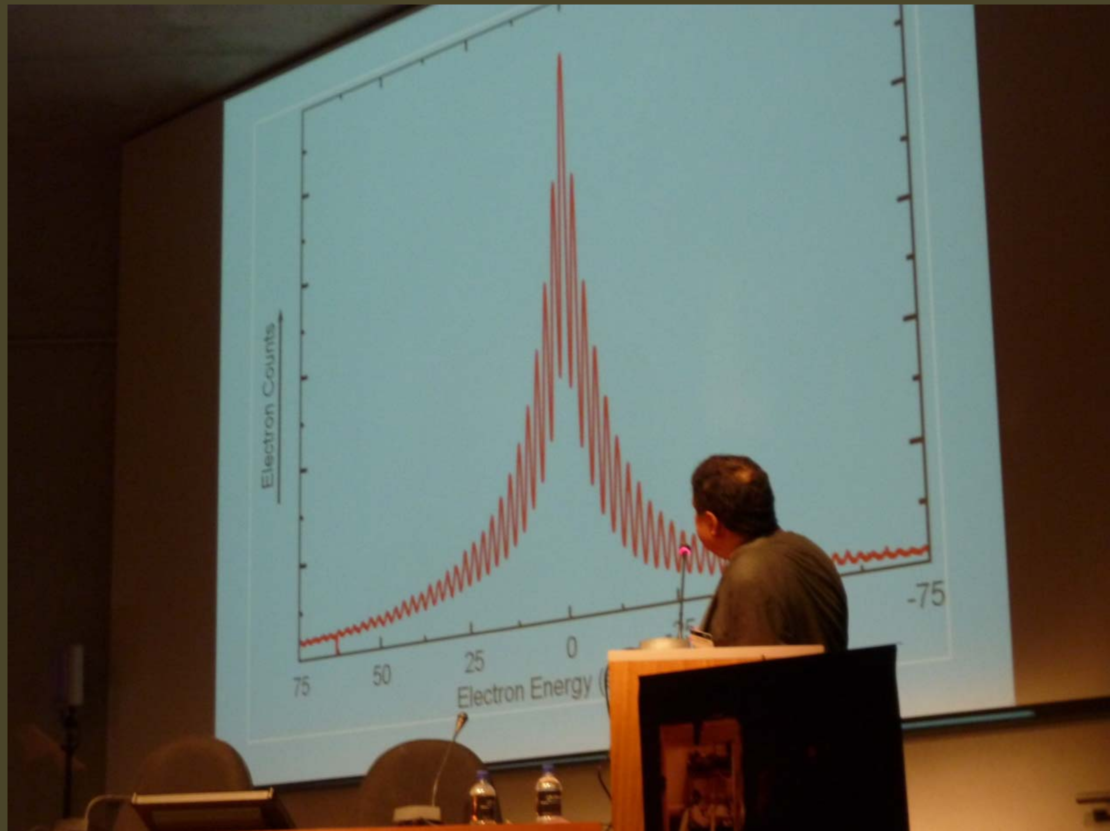

and now?

With synchronised light injection (cf Zewail's group at UCLA)

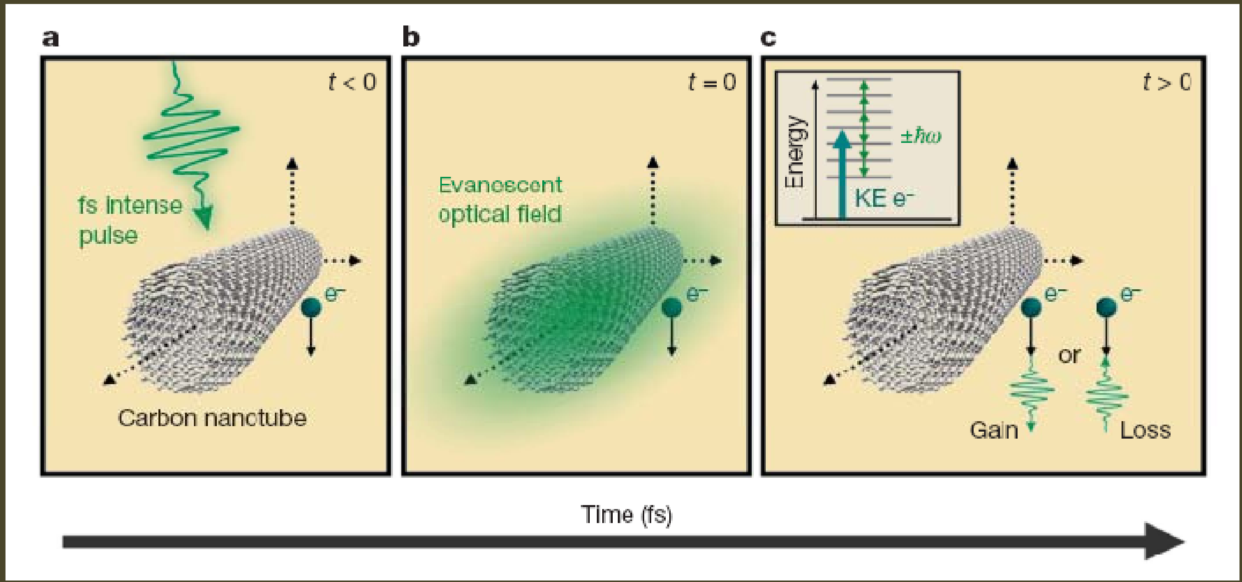

New spectroscopies synchronizing electrons and photons (injecting light)

•(i) electron energy-GAIN spectroscopy

•(ii) dynamics of excited states

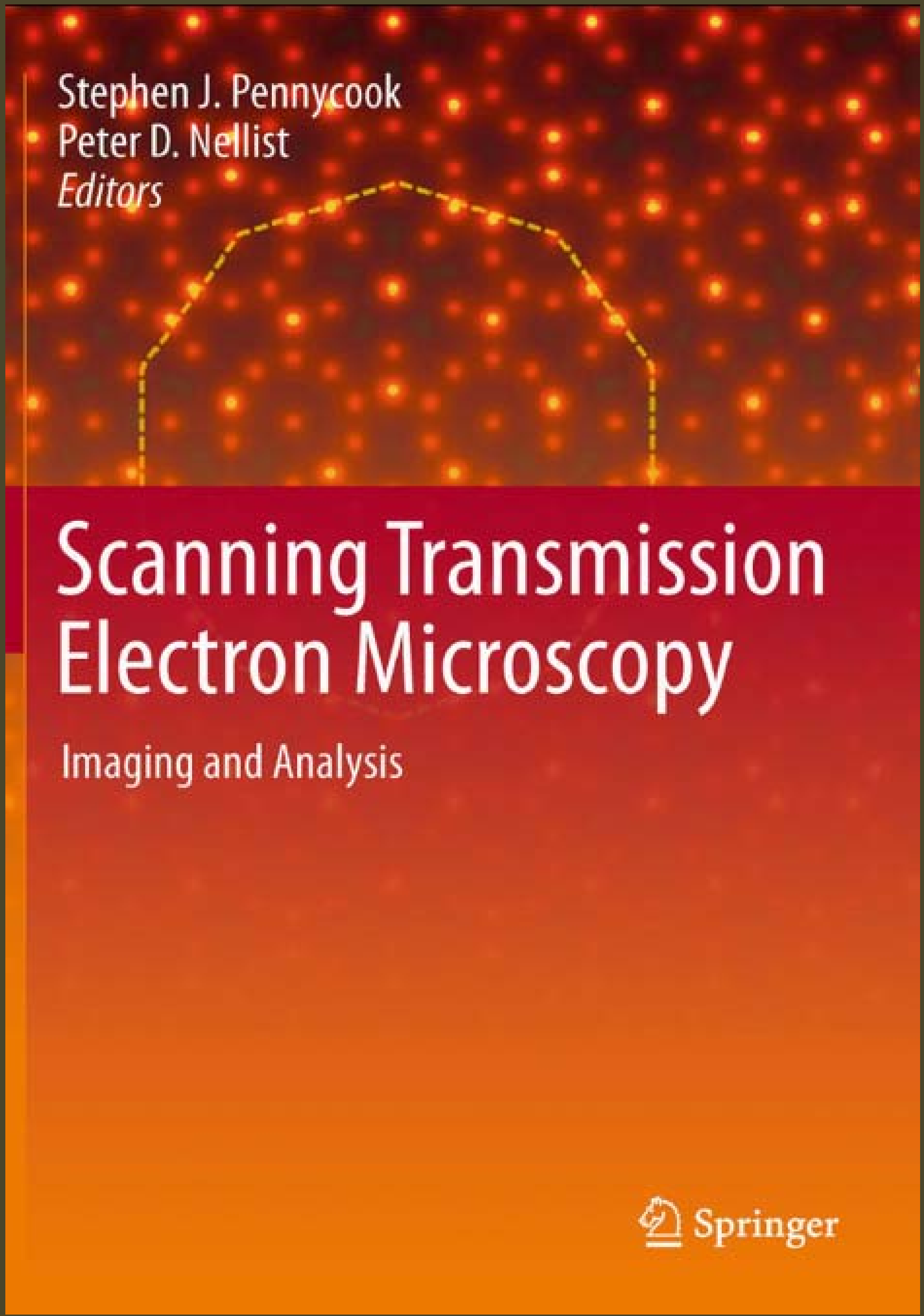

The most recent textbook on the market…

MRS Bulletin, january 2012
on
"Spectroscopic Imaging in Electron Microscopy"

Eds. S. Pennycook & C. Colliex

Invited contributions :

G. Botton, McMaster, Canada
M. Varela et al. ORNL, USA and Madrid, Spain
M. Kociak, Orsay, France & J. Garcia de Abajo, Madrid, Spain
K. Suenaga et al. AIST, Japan
L.J. Allen et al. Melbourne, Australia
M. Aronova & R.D. Leapman, NIH, USA

dépasser les frontières

LPS ORSAY

Laboratoire de Physique des Solides · UMR 8502 Université Paris sud bât 510 · 91405 Orsay cedex

UNIVERSITÉ PARIS SUD

Comprendre le monde, construire l'avenir®

The Orsay team enabling the future (june 2011)

http://www.lps.u-psud.fr/stemlps

Thanks to all my colleagues at LPS Orsay

Guillaume Boudarham, Laura Bocher
Nathalie Brun, Alexandre Gloter,
Mathieu Kociak, Katia March,
Stefano Mazzucco, Claudie Mory,
Odile Stéphan, Marcel Tencé,
Almudena Torres-Pardo, Mike Walls,
Luis Zagonel and Alberto Zobelli
from LPS Orsay, France

Thanks to CNRS CNRS and to EC funded programs EU SPANS et ESTEEM and to all our partners who have submitted scientific issues to solve and suited specimens

Thank you very much for your attention